

## Supplementary Material

## What the supplement is about

In this supplement we collect a number of explanations and/or elaborations on technical issues, as well as some illustrative material that could not find a place in the main article.

Most figures in this supplement are actually referenced in the article. It is expected that the reader of the supplement is familiar with the material discussed in the article.

Anyone intending to use the methods discussed in the main article will benefit from consulting the supplement in addition.

Most of the material discussed here will not be found neither in current textbooks, nor in the current English literature. Some of the material is based on pre–WW–II literature of continental Europe (including Russia). The language was mainly German, but also a variety of other languages. Most of it was never translated. The few works that were translated tend to attract the interest of historians of science, rather than active researchers in the field of color.

Some of this corpus dealt with the rigorous, formal structure of colorimetry. An example is Erwin Schrödinger's fundamental work, which has actually made it into the better modern textbooks. Most of the heritage had to remain largely on the level of intuitions or heuristics, although some was exploited in actual applications. The key example is Wilhelm Ostwald, which is the more remarkable because Ostwald conceived of, and backed up his ideas with observations involving actual optics instead of mere virtual reality. There was no computer graphics or image processing at the time.

The use of computers enables one to really exploit such heuristics and integrate them in the formal framework of colorimetry. This yields an account of colorimetry that goes beyond the contemporary conventions.

E.Schrödinger (1920). Theorie der Pigmente von größter Leuchtkraft. Annalen der Physik 4(62), 603–622.

E.Schrödinger (1925). Über das Verhältnis der Vierfarben- zur Dreifarbentheorie. Sitzungsberichte der Akademie der Wissenschaften in Wien. Mathematisch-naturwissenschaftliche Klasse, Abteilung 2a. 134, 471–490.

<sup>2</sup> Se

W. Ostwald (1919). *Einführung in die Farbenlehre*. Unesma, Leipzig; W.Ostwald (1917a). *Die Farbenfibel*. Unesma, Leipzig.

W.Ostwald (1917b). Der Farbatlas. Unesma, Leipzig.

<sup>1</sup> See:

## 1 DISPLAY

Eventually almost any colored image will end up as RGB. One might prefer CIE XYZ, CIE Lab, HSB, or whatnot, but when the rubber hits the road the display hardware will be driven by RGB signals.<sup>3</sup>

As argued in the article, RGB is not only a de facto final format for display. It is actually a colorimetric (geometrical) description of colors that is closely related to spectral reflectance factors of materials under more or less "standard" lighting conditions. This renders RGB the preferred description for object colors.<sup>4</sup> It was the natural choice for the founders of colorimetry, Maxwell and Helmholtz, in the nineteenth century and for very good reasons. As we argue in the article, it lets one deal with physical material properties and radiant sources of illumination, as well as with various effects of metamerism in a principled manner.

However, the display stage is of conceptual and practical interest as a topic by itself. The article is not primarily about that, but here we discuss a few aspects that are related to the topics treated in the article.

## 1.1 Standard presentation of object colors

An effective way to present object colors is shown in fig. S1. Of course, these are only "object colors in virtual reality," because presented on an electronic display, luminous surfaces instead of illuminated surfaces. That is a fundamental difference.

Thus you cannot present a uniform patch that looks "golden." However, you can effectively present browns, olives and grays, whereas these have no existence as luminous (or "beam") colors. That this is possible is due to the embedding in a minimum context.

Apart from providing a context, one also needs to avoid possible effects of simultaneous contrast, assimilation, and so forth. The example shown here should prove generally useful.

The overall background is gray on the average, like the immediate surround. White and black patches anchor the scale.<sup>5</sup> The fiducial color is seen in isolation (due to the average

<sup>&</sup>lt;sup>3</sup> For printing that might be CMYK, but that is not a fundamental difference.

<sup>&</sup>lt;sup>4</sup> Do not confuse this with the CIE RGB 1931 color space, there is no relation. Wright and Guild did colorimetry in the 1920's, using three monochromatic primaries at standardized wavelengths of 700nm (red), 546.1nm (green) and 435.8nm (blue). They were not interested in object colors, the CIE RGB space has the same ontological roots as the CIE XYZ space.

<sup>&</sup>lt;sup>5</sup> A.Gilchrist (1999). *Lihtness Perception*. In: R.A. Wilson and F.C.Keil, (Eds), MIT Enclyclopedia of Cognitive Science. Cambridge: MIT press, pp 471–472.

gray annulus), is properly anchored and is hardly effected by simultaneous contrast.<sup>6</sup> Adaptation still occurs,<sup>7</sup> so one should not stop to scan the eyes over the pattern.

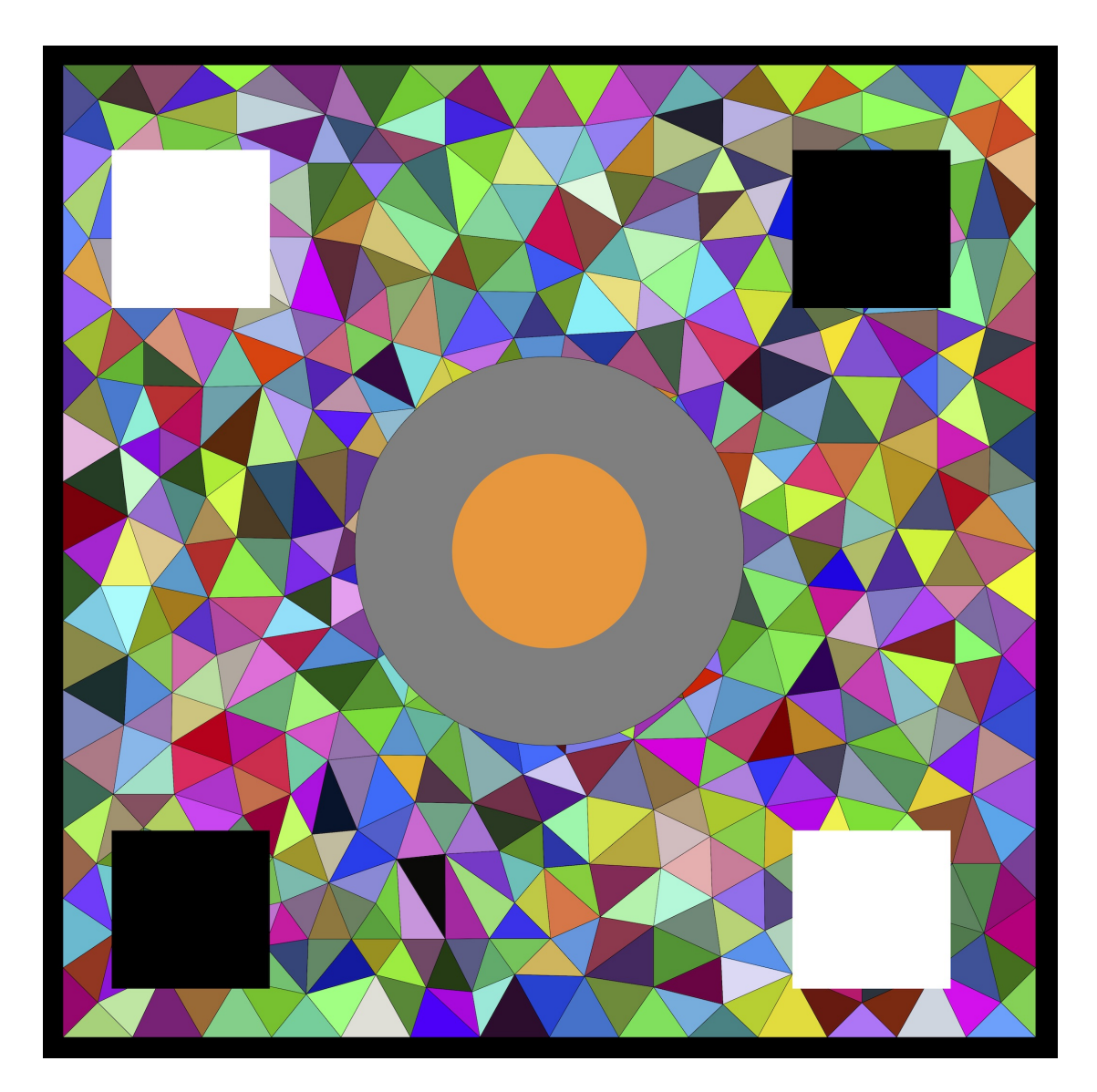


**Figure S1.** An effective way to present "object colors." In this case the color that is presented is an orange. It is presented in the central disk. The remainder of the display serves to present context and suitable anchoring of the scale. In viewing the patch one should avoid fixation of the central disk, but move the eyes over the image in a natural manner.

<sup>&</sup>lt;sup>6</sup> W. von Bezold (1874). *Die Farbenlehre in Hinblick auf Kunst und Kunstgewerbe*. Vieweg, Braunschweig.

<sup>&</sup>lt;sup>7</sup> K.Hirakawa and T.W.Parks (2005), Chromatic adaptation and white-balance problem. Conference Paper in: Proceedings / ICIP International Conference on Image Processing 3:III – 984-7 – October 2005, 4 pages.

This patch appears like a  $\sharp$ tint (it contains some  $\sharp$ white) of  $\sharp$ orange to us. With some experience one might estimate RGB[99|60|20]. Mismatches occur if there are differences of the order of 05 (the range is 00–99) in the usual RGB display coordinates. Because of the anchoring the illuminant (in print) or display calibration (on a screen) are not all that crucial.

## 1.2 Display colors

Colors may be displayed in many ways. Think of paint, print, silverhalite photography, electronic displays, . . . . Technologies come, technologies go.

Physical display uniquely communicates color. Science, concepts and language are all important, but are equally unable to communicate color. Color as quale is an emphatic, not conceptual, mental strand of *Homo*.

Technology constrains formal description. In a phosphors based display (old-fashioned TV-set) one moves towards the center of the color solid by attenuation and adding white (one gets black for free). In contradistinction, in printing with transparent inks one adds black (one gets white for free). In human perception black and white play equivalent, mutually complementary roles.

In a display based on three basic colors that can be combined additively, the RGB tripartition discussed in the article yields the unique optimum choice for the primaries (fig. S7). The display ostensively defines  $\sharp$ **colors** by way of the contraction map  $\Downarrow$ .

Formal object color colorimetry yields RGB coordinates. Most are in the range 0...1, thus can be displayed without further ado.

The rare under— and over—shoots are (typically *much*) less than 20% (rarely exceeding 1%). In typical databases a few colors (say a few percent) may over or undershoot, typically by less than a few percent.

The common "solution" is clipping. More accurate is to project on  $\mathbb{I}^3_{rgb}$  from the center of the color solid. It is unlikely that the difference would be spotted.

#### 1.3 Calibration issues

Display units are supposed to be linearized and radiometrically calibrated. Most at least approximately are. Over and above this, one uses (nonlinear) "gamma correction" to accommodate human vision, encapsulated in hard and software. The user specifies color coordinates, say RGB[99|66|20] (programmers will prefer hexadecimal notation of triple-byte values #FF AA 33 and expect a certain variety of #orange ( ) on the screen).

Effects of the gamma correction may be confusing, depending on the soft—and hard—ware environment. For instance, the center of the color solid has coordinates RGB[50|50|50|, which looks a #**light gray**. An apparent #**middle gray** will have an albedo of about 20% (not 50%). Yet when we use "RGBColor[0.5,0.5,0.5]" (fairly generic type of command) in Mathematica<sup>©</sup> we get a nice #**middle gray** on the screen. Setting the gamma to 1 (linear display) counteracts that.

Unknown software (especially when "under the hood") should be checked for effects. In many cases eye measure will solve a problem, otherwise one turns to spectroradiometry.

The colors in this paper were obtained by feeding the colorimetric coordinates in standard "RGBColor[\*,\*,\*]" commands in Mathematica on a MacBook Pro (Retina, 15–inch, Mid 2015) platform using factory settings. Radiometric monitoring shows this to be acceptable. Unfortunately, we have no control on what happens at the publisher, or on a reader's display.<sup>8</sup>

## 1.4 Transformations between color spaces

All simple (just colorimetry, no arbitrary conventions) color spaces are equivalent although some are far more natural and intuitive than others. It is a trivial matter to transform between them. Setting up the transformation is only a matter of expressing the primaries of one system in that of the other.

For instance, in order to transform between  $\mathbb{C}_{RGB}$  and  $\mathbb{C}_{xyz}$  and vice versa, one may use  $(T_{RGB}^{XYZ} \text{ from RGB to XYZ}, T_{XYZ}^{RGB} \text{ the other way})$ :

$$T_{\text{RGB}}^{\text{XYZ}} = \begin{pmatrix} 0.23490 & 0.27642 & 0.89303 \\ 0.09477 & 0.76505 & 0.54501 \\ 1.29465 & 0.11032 & 0.00005 \end{pmatrix}, \qquad T_{\text{XYZ}}^{\text{RGB}} = \begin{pmatrix} 0.05654 & -0.09269 & 0.50113 \\ -0.66394 & 1.08791 & 0.04083 \\ 0.92221 & -0.31236 & -0.14445 \end{pmatrix} \tag{S1}$$

(For the case of object colors any constant factors will cancel out if the computations include automatic white balance.) It is often useful for graphical representations, as many people prefer CIE XYZ over RGB because it is considered scientifically respectable.

Transformations are not always simple, or even possible in more complicated representations that depend on arbitrary conventions from outside colorimetry proper. This may influence the choice of a representation. For instance, it is not really possible to handle subtractive mixture or metameric effects in such systems as CIE Lab, 9 so if the interest is of a biological nature one had better avoid it.

<sup>8</sup> In order to obtain some notion of what might happen — due to a variety of factors — one may collect a few dozen variations on a well known painting from the Internet. Pairwise side-to-side comparison will reveal highly noticeable variations.

<sup>9</sup> CIE Lab defined via an awkward non-linear transformation, so it is not fit for colorimetric calculations. In order to achieve that one needs continual transformations back and forth. Formal work is so unwieldy as to be practically impossible.

## 1.5 About the colors in the figures

In the RGB-description the color coordinates can double as the usual display RGB-coordinates, except for the usual gamma correction. Thus many of our figures were colored in this way. It has the advantage that one immediately sees the coordinates when looking at the figure, something that is impossible, or would need some extensive training, in terms of the more conventional descriptions.

We use RGB-coordinates straight when all coordinates are in the zero to one range. Coordinate over- or under-flow is handled by hard clipping. This occurs with object colors that are outside the RGB-cube, but inside the color solid. The under- and over-shoots are necessarily small, the effect of clipping is essentially unnoticeable.

Problems also occur occasionally with radiant spectra shown as object colors. In such cases we scale the coordinates so the maximum coordinate value equals one. Although an ad hoc convention, it is the best one can do. It may lead to confusion because a monochromatic 700nm reflectance will look black as an object color, whereas this convention will represent it as a red. Radiant spectra cannot be displayed as object spectra, except by way of some arbitrary convention. This applies to figure \$30.

Some figures are colored where the color only has an indicative meaning. Colors in these figures should NOT be interpreted as RGB—coordinates as intended in the paper. In most cases that will be immediately obvious from the context. However, in order to avoid misunderstandings, these are the figures 1, 2, 5 top and bottom right, 7–10, 12 left, 17, 19, S1, S7–S9, S12, S13, S15–S19, S22, S25–S28, S35–S37 and S43–S46.

Of course, we cannot guarantee "fully calibrated" results in print or on the Internet. However, we reckon that the figures are good enough to prevent confusion. The advantage is clearer, more useful figures. It is also useful as a correction on common usage, the many painted CIE-XY chromaticity diagrams used to indicate object colors. Such diagrams actually show equivalence classes of radiant spectra of arbitrary radiant power, thus rendering a unique mapping on display colors impossible.

## 2 THE SHARP MAP

The "sharp map"  $\sharp$  is defined via the psychogenesis  $\Psi$ :

$$\{\Psi : \mathbb{C} \leadsto \mathbb{Q} \mid \Psi(\mathsf{RGB}[99|00|00]) = \sharp \mathbf{red}\}, \quad [\text{the "sharp}(\sharp) \, \mathrm{map"}], \quad (S2)$$

is often considered problematic because the very "existence" of psychogenesis ( $\Psi$ ) and qualia  $\mathbb{Q}$  are denied by physicalists. (On the issue of "Color appearance" see Fairchild, M.D. (2013). Color Appearance Models, John Wiley & Sons, West Sussex, UK.)

Such a view is rather myopic in view of the following facts:

It is no problem to determine the structure of the map empirically. The probability of confusing  $\sharp \mathbf{color} \mathbf{A} = \Psi(A)$  with  $\sharp \mathbf{color} \mathbf{B} = \Psi(B)$  can be measured in an objective (behaviorist) manner. The structure of the  $\Psi$ -map in terms of the domain  $\mathbb C$  can be measured objectively with observers acting as null-detectors in the range  $\mathbb Q$ .

With color naming as criterion about a dozen **#colors** are distinguished. With a production method (bypassing conceptual, linguistic thought) this number rises to the hundreds. This is still far less than the number of physiologically discriminable colors, estimated as up to forty million.<sup>10</sup>

In any specific application one should decide what the expected fuzziness of the sharp map is. For critical applications one may assume 0.01–0.02 in the RGB coordinates on a 0–1 scale. For most user applications that is excessive and one may assume a fuzziness of 0.1–0.2. That would apply to a "standard presentation." If the context is very different the deviations may become much higher and — perhaps worse — systematic instead of random.

In most applications the fuzziness may be treated as isotropic. However, differences between the teals and the oranges, etc., are certainly present, even on the 0.1–0.2 level. 11

<sup>10</sup> See:

D.L.MacAdam (1942), Visual sensitivities to color differences in daylight. JOSA 32(5): 247–274.

G.Wyszecki and W.S.Stiles (1967), Color science: Concepts and methods, quantitative data and formulae. Wiley, New York.

<sup>11</sup> See:

J.J.Koenderink, A.J. van Doorn and K.Gegenfurtner (2018), *Graininess of RGB-Display Space. i-*Perception 9(5), 1–46. and

J.J.Koenderink, A.J. van Doorn and K.Gegenfurtner (2019). Colour Order. i-Perception 10(4), 1–12.

## 3 SUBTRACTIVE COLOR MIXTURE OF THE CARDINAL COLORS

The subtractive color mixture of RGB colors is especially simple to understand for the case of the cardinal colors. The spectral reflectance factors are characteristic functions and the transition loci are fixed, so we can simply multiply the RGB coordinates: it amounts to the same as intersecting the spectral regions. Thus the subtractive mixture table boils down to

	100					
100	100	100	000	000	001	100
110	100 100	110	010	010	001	100
010	000	010	010	010	000	000
011	000	010	010	011	001	001
001	000	000	000	001	001	001
101	100	100	000	001	001	101

This is illustrated in fig. S2. Of course, the set of cardinal colors is periodic, so the "natural" representation is on the torus. (We use a mirror to view the lower side too.)

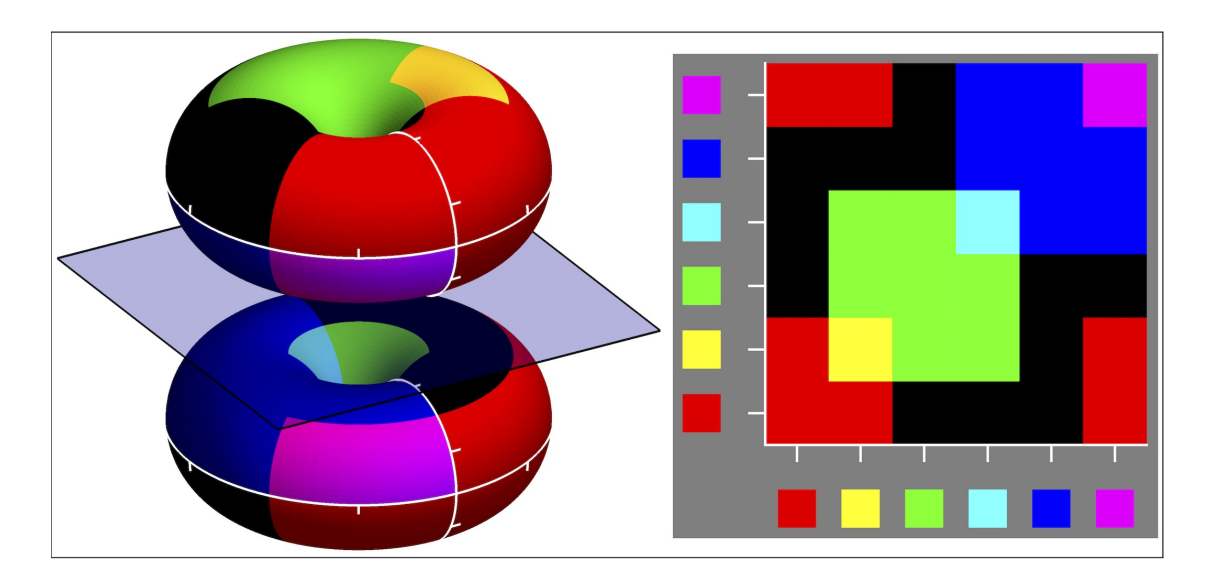


**Figure S2.** Subtractive color mixtures of the cardinal colors. The "horizontal" axis of the left and right figures are the same, so are the "vertical" axes. In the case of the torus the axis are obvious closed, in the case of the square at right that is not immediately obvious. (Ignore the fact that the scales of the axes on the torus are necessarily unequal.)

## 4 THE EDGE, OR BOUNDARY COLORS

The edge colors, or boundary colors, are basic for the object colors, as any point on the boundary of the object color solid can be represented as the difference of two boundary colors, or — what amounts to the same — a chord of a boundary color curve.

The boundary color loci are smooth curves that run between the white and the black apex of the color solid. They are twisted curves, irregular helices of half a turn (fig. S3).

Different from the spectrum, which is essentially invisible for the object colors (each spectral component has infinitesimal intensity), the boundary colors are easily displayed. You can see them by looking at a black-white edge through a prism, that is how they were disovered by Goethe. fig. S4 yields an impression.

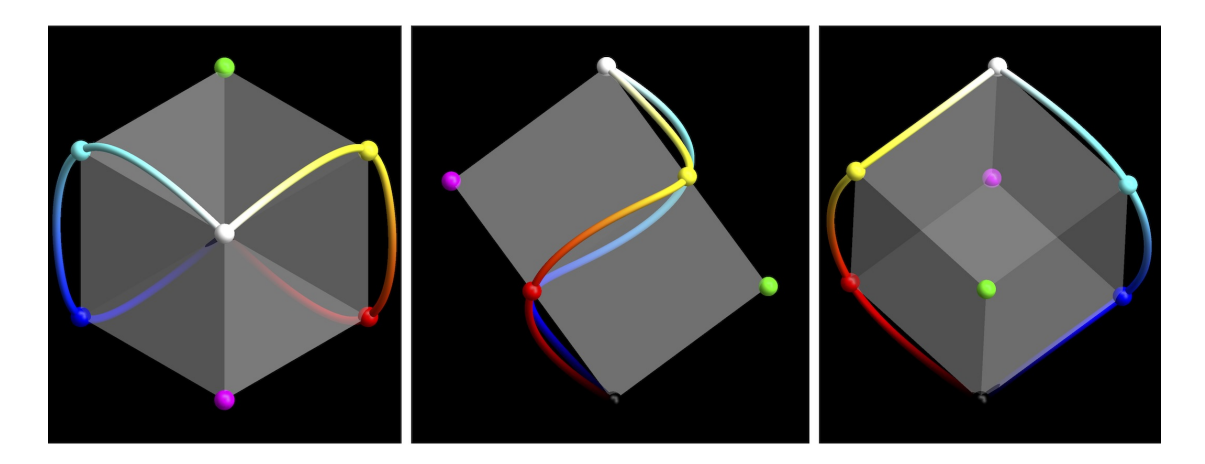


**Figure S3.** Different (orthographic) perspectives of the edge–color series plotted as curves in  $\mathbb{C}_{RGB}$ . The view from the achromatic direction (left) is perhaps the most informative. This figure also shows the intimate relation to the unit cube. (For colors see fig. S4.)

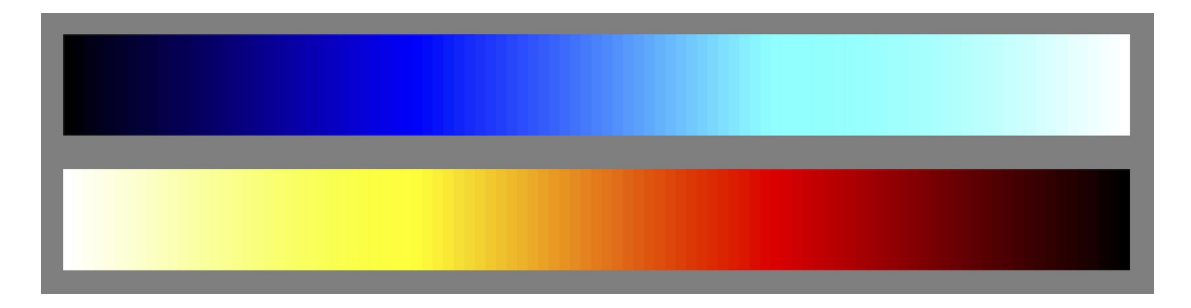
The two boundary spectra are mutually complementary, for geometrically they are related through the central symmetry of the color solid.

Figure S3 shows three mutually orthogonal orthographic views of the boundary color loci. It also reveals their relation to the RGB cube.

The warm boundary color sequence is black—red—yellow—white, whereas the cool sequence is white—cyan—blue—black. That is orange and teal. <sup>12</sup> Note that the curves run outside the RGB cube, that is because they lie on the surface of the color solid. However, their relation to the RGB—cube is seen to be very intimate.

<sup>12</sup> J.J.Koenderink and A.J.van Doorn (2020). Orange & Teal. Art & Perception, in press.

That the boundary colors provide the natural interface to the spectral properties is due to the fact that the correlation length of the spectrum envelope of the spectral reflectance functions of natural materials is dominated by the spectral slope. This causes object colors to cluster about the boundary color loci in the RGB cube. The result is a dominance of teal-oranges (spectral slope) over purple-greens (spectral curvature), which is evident in databases of spectral reflectance factors, RGB colors and the statistics of images of natural scenes.<sup>13</sup>



**Figure S4.** Impression of Goethe's *Kantenspektren*. The colors are just the displayed values of the accumulated spectral components of white. (These two spectra are "supplementary," they mutually add to white. Supplementary implies "complementarity," a weaker concept.)

<sup>13</sup> See: J.J.Koenderink and A.J.van Doorn (2017). *Colors of the sublunar. i-*Perception, 8(5), 1–30. and

J.J.Koenderink, A.J. van Doorn and K.Gegenfurtner (2020). Colors and things. i-Perception 11(5), 1-43.

# 5 SCHOPENHAUER'S BIPARTITIONS OF THE SPECTRUM AND THE OPTIMUM TRIPARTITION

Arthur Schopenhauer noticed the fact that the colors obtained by splitting the spectrum of white into two adjacent parts are especially striking for just a few bipartitions. That can be seen in this illustration (fig. S5):

## Schopenhauer style bipartitions

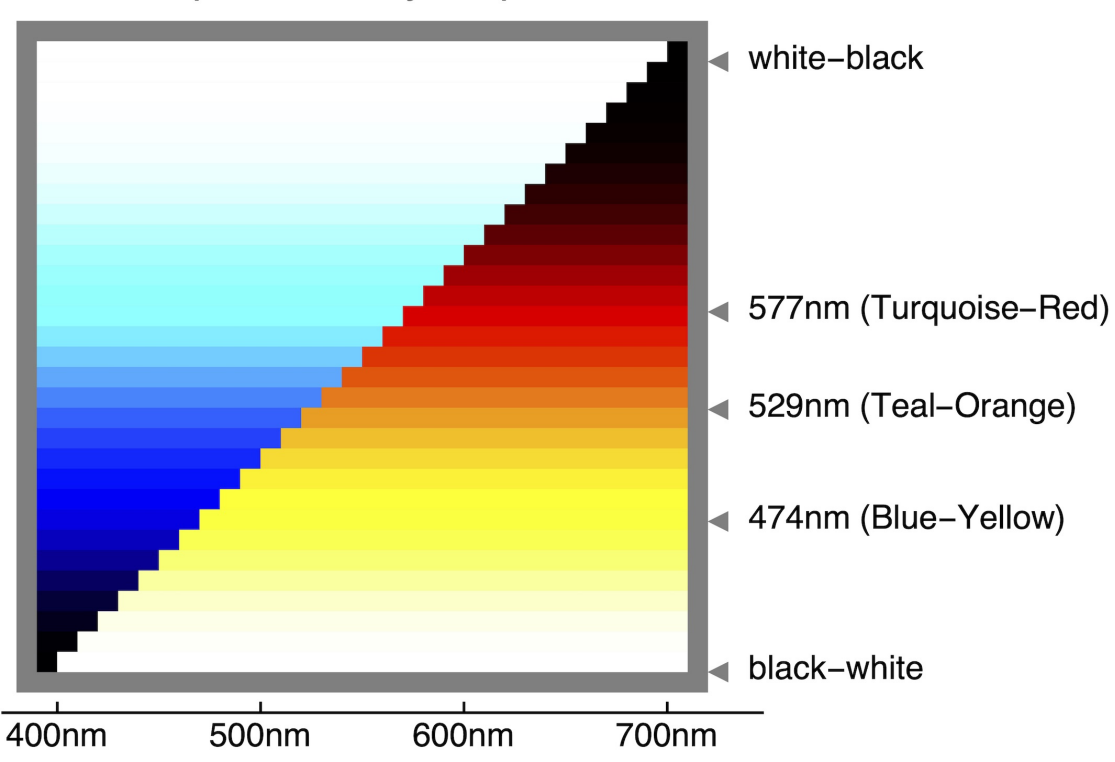


**Figure S5.** Schopenhauer-style bipartitions of the source spectrum  $\mathcal{E}(\lambda)$ .

Illustration fig. S6 shows Schopenhauer's analysis. His color terms are:

Schwarz black

**Violett** he apparently indicates blue, the complementary of yellow

Blau he apparently indicates teal, the complementary of orange

Grün green, here apparently a cyanish green

Roth red, but here apparently purplish red

Orange orange

Gelb yellow

Weiss white

Whether Schopenhauer's red-green is turquose-red or green-purple (or something in

## Aus meiner Darstellung ergiebt sich folgendes Schema:



**Figure S6.** Schopenhauer's original scheme. Notice the fractions. In terms of RGB yellow:blue would be 2/3 : 1/3, green:red 1/3 : 1/3. How Schopenhauer arrived at the fractions is unclear.

between) is hard to say. See for yourself. In the illustration we indicated white-black, turquoise-red and teal-orange. It is "visually evident" that there are indeed "best cuts" though.

Because Schopenhauer's cuts overlap, he really indicated a tripartition. For a spectral tripartition one may suggest a formal criterion: the largest inscribed crate in the color solid. The definition is (as should be!) affinely invariant. It is expected to yield a unique crate. The way to check is by exhaustive search (fig. S7).

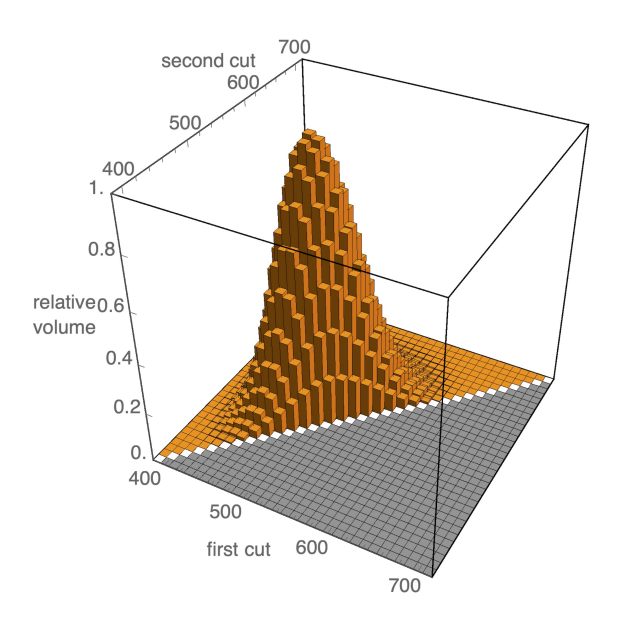


**Figure S7.** Dividing the spectral range into three parts yields three colors, the three colors span a volume. Here that volume is plotted as a function of the spectrum cut loci. There exists a unique optimum.

The expectation is apparently validated. There exists a pronounced optimum.

It is of some interest to consider the tripartition for the contraction and expansion maps as defined in the main manuscript (fig. S8).

The tripartition induced by the crate gives rise to a number of relations that are of some interest figs. S9 to S11.

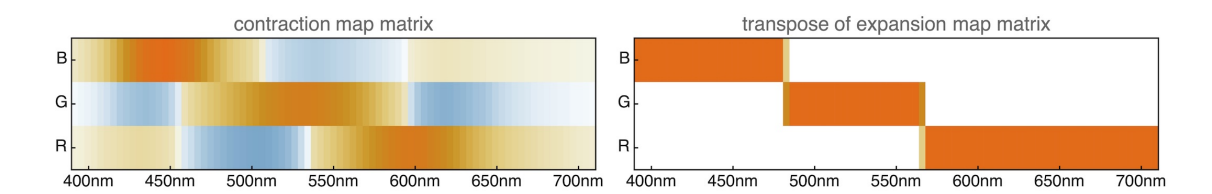


**Figure S8.** The contraction and expansion maps have intuitively obvious matrix representations. The rows of the contraction map matrix are the color matching functions. The columns of the expansion map matrix are the characteristic functions of the parts of the optimum tripartition. (We plot the transpose to save space.) Colors are contracted spectra, canonical spectra are expanded colors. Unlike CIE  $\mathbf{M}_{\mathrm{XYZ}}$  these matrices are intuitively structured.

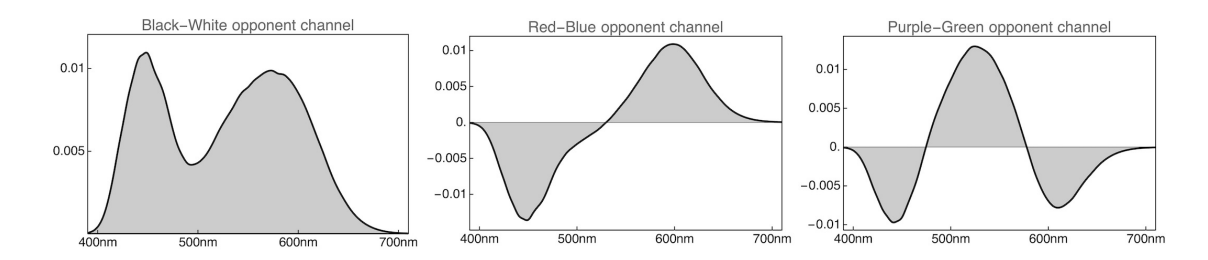


**Figure S9.** These are the "Hering opponent channels." They correspond to the  $\{h_1, h_2, h_3\}$ -basis. The  $h_2$  effectively computes a first order derivative (slope) of the spectral envelope, whereas  $h_3$  computes the second order derivative (curvature) of the spectral envelope. That is what color is in a biological, evolutionary sense.

The Hering components (fig. S9)<sup>14</sup> are an RGB related representation in which the spectral mean, slope and curvature are given a key role. Although this representation was originally derived from purely phenomenological arguments, it is actually quite close to the natural representation from ecological physics.

<sup>14</sup> E.Hering (1905–1911). Grundzüge der Lehre vom Lichtsinn. Sonderabdr. a. d. Hdb. d. Augenheilkunde. Voss, Leipzig.

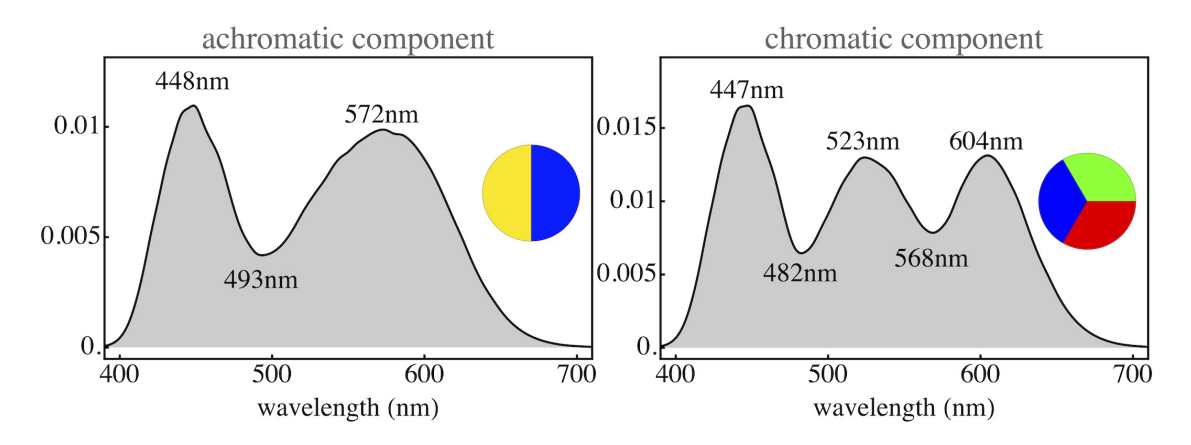


**Figure S10.** Two different projections of the edge–color series. At left a projection on the achromatic axis (essentially the black-white Hering opponent channel (fig. S9)). It is bimodal. At right the length of a projection on the plane orthogonal to the achromatic direction. It is trimodal.

The two— or three—peaked graphs (fig. S10) are frequently encountered in various regions of classical color science. In many cases the authors are puzzled and try to argue in the direction of an overall unimodal shape — like the CIE luminance function.<sup>15</sup>

The angular rate with wavelength (fig. S11) is of interest because it clearly indicates that the wavelength is just an arbitrary continuous parameter. Wavelength is not relevant with respect to object color. The way to deal with this in a principled manner was intuited by Wilhelm Ostwald in the early twentieth century.

<sup>15</sup> CIE (Commission Internationale de lÉclairage) (1932). Commission Internationale de lÉclairage proceedings 1931. Cambridge University Press, Cambridge, UK.

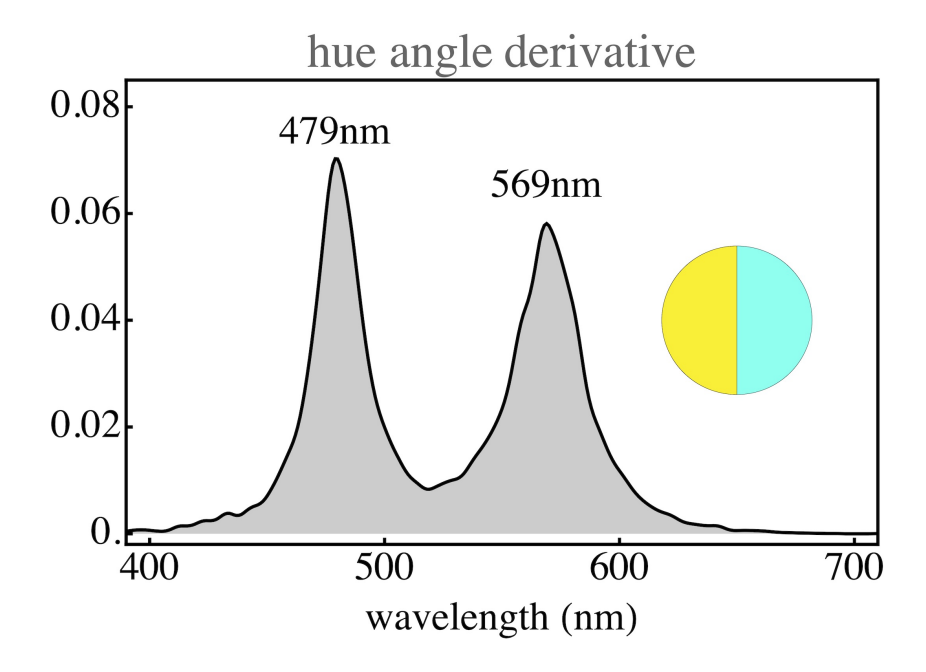


**Figure S11.** In spectral ranges near 479nm (cyan) and 569nm (yellow) the angle parameter varies especially fast with wavelength.

## 6 THE SEMICHROME LOCUS

The red line in fig. S12 is the semichrome locus. Thus the semichromes are the "equator" of the color solid and have the highest possible chromaticity. Note the relation to the boundary colors (yellow) and the shape of the lines of equal achromatic content in the chromaticity diagram.



Figure S12. Lines of equal achromatic content in the chromaticity diagram.

The semichromes are easily computed because their transition loci are mutually complementary. Here is a diagram (fig. S13) that is more "traditional" than the (much nicer!) one printed in the manuscript:

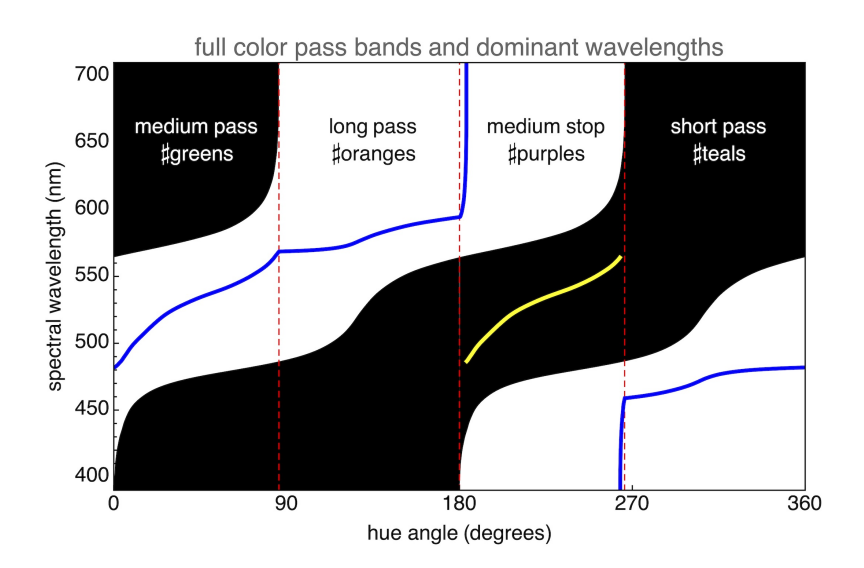


**Figure S13.** This is the Ostwald diagram in more conventional form. (The extra-spectral part shown in fig. S19 has been omitted.) Note the partition into short pass, medium pass, long pass and medium stop spectral reflectance functions. These correspond to the **#teal**, **#green**, **#orange** and **#purple** object color families. This tetra-partition might be called "Hering partition" It is different from the tri-partition based on the optimum crate.

We consider a few more perspectives on the semichromes (figs. S14, S15, and S26).

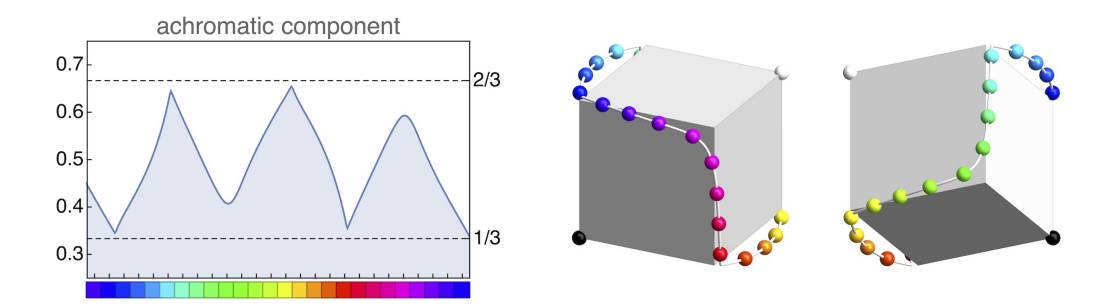


**Figure S14.** At left, projection of the semichrome color curve on  $\mathbf{h_1}$  reveals six locations that visually stand out. They come as two triples. These correspond to the chromatic vertices of  $\mathbb{I}^3_{RGB}$ . Note that the hue range is — different from the spectral range — periodic! At right a string of 24 beads of semichromes is plotted next to the cube. The curve closely hugs the R-Y-G-C-B-M-R-edge progression.

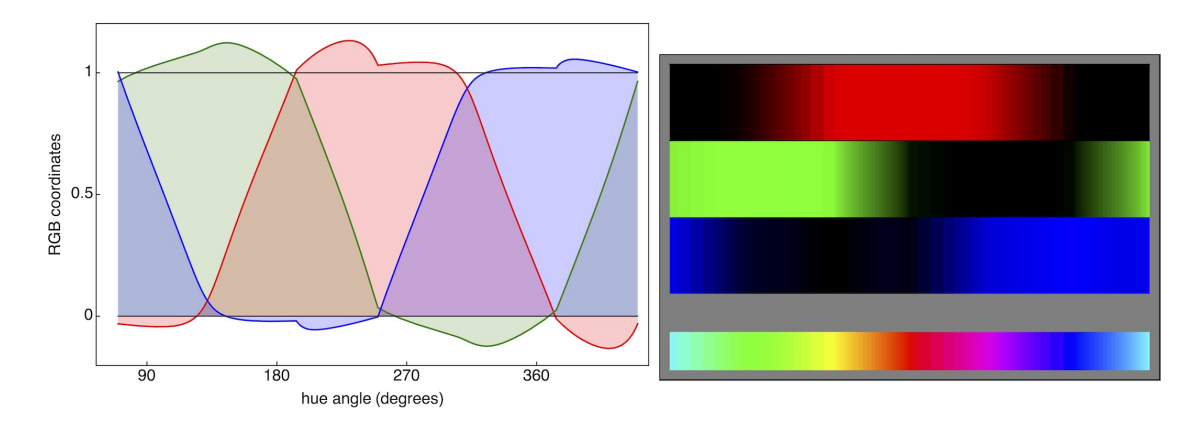


**Figure S15.** At left the RGB—coordinates of the semichromes as a function of hue angle. Note the over and undershoots. At right the red, green and blue parts of the semichrome colors. Find the four families!

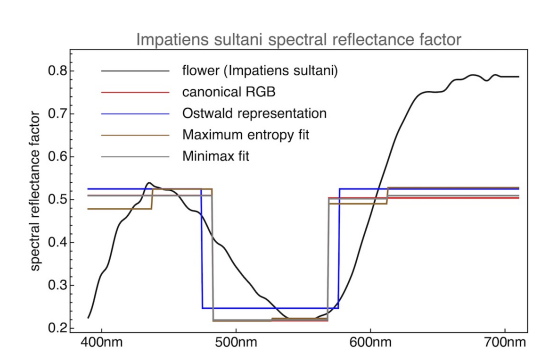
Figure S14 shows that the semichromes are closely related to the RGB cube. They form the periodic sequence red-yellow-green-cyan-blue-violet-(red), but – of course — run strictly outside of the RGB-cube. After all, they lie on the surface of the color solid. If you consider the projection on the achromatic axis, you clearly see that the so called "cardinal" colors are indeed *special*. It is also evident that they come in two types: the "primary cardinal colors" red, green and blue, and the "secondary cardinal colors" cyan, magenta and yellow. The primary and secondary cardinal colors are mutually complementary, those pairs are just the Schopenhauer bipartitions (section 5).

Figure S15 plots the RGB coordinates of the semichromes. If you shave off the underand over—shoots, you get the familar RGB implementation. This once again shows the close connection between the RGB coordinates and the color solid.

## 7 CANONICAL SPECTRA

What is a "canonical spectrum" for an RGB color? Since there are infinitely many choices — except fot the colors on the boundary of the color solid — it is essentially up to you to take your pick! However, some choices are far more useful than others. But, as expected, the proper choice depends upon your context.

In our option the canonical spectrum based on the optimum tripartition wins hands down in almost any case. However, there is certainly something to say for Ostwalds' choice. Fortunately, in most cases the choice doesn't really make all that much difference. fig. S16 show a typical case.



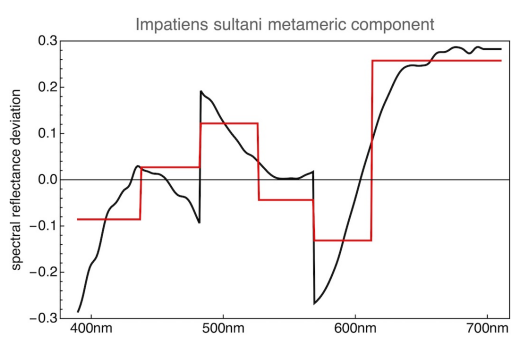


**Figure S16.** A fairly typical case. Here the spectral reflectance factor of a violet flower has been approximated in various ways. Notice that the canonical spectra (either tripartite or Ostwald) do a good job of capturing the bulk of the action. The minimax and maximum entropy (section 10) are fairly close too. The metameric component is well captured by the difference between the true spectrum and the tripartite canonical spectrum (say). A simplification is to project that on the three metameric blacks (section 12), shown at right. Here the black curve shows the metameric difference with the canonical spectrum, the red curve the projection.

So what to do? In practice, you may want to decide on the basis of the structure of the description. Figure S17 compares four obvious contenders.

The Schrödinger representation<sup>16</sup> is the one that would be picked by a physicist (Schrödinger!) without so much as thinking twice. It is also popular with mathematicians and theoreticians dealing with colorimetry. That is because the description centers on what immediately hits the eye, that is the beam scattered by the object. It is just barely possible to speak of "object color" by introducing a unit level, that of a white reference object. This is essentially the choice of the (majority) of vision scientists who will strongly recommend CIE LAB. Such people have a hard time to accept black as a "real" color. That is because to a physicist black is *nothing*.

<sup>16</sup> E.Schrödinger(1920), Theorie der Pigmente von größter Leuchtkraft. Annalen der Physik 4(62), 603–622.

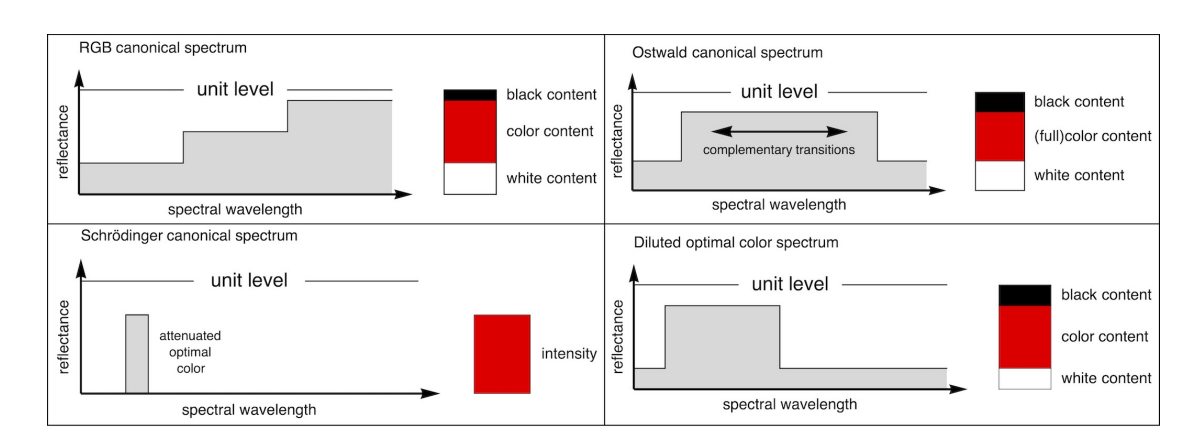


**Figure S17.** Some useful "canonical spectra." Top left the tripartion of white. Top right Ostwald's proposition. Bottom left Schrödinger's attenuated optimal color. Bottom right an interpolation between central gray and an optimal color. In all cases one may speak of color, black and white contents, although the meanings would differ. Schrödinger would not have used "black content" but would prefer to speak of an attenuated spectrum. Black and white only make sense in the generic object color context, they are meaningless in generic (context-free) colorimetry.

Phenomenologically black is not less real than white. That was Hering's (psychologist) opposition to Helmholtz (physicist).<sup>17</sup> The point of friction is that black and white are mental entities, whereas dark and bright (when suitably defined) are physical entities. It is the old notion of Goethe that color is where the mind meets the world.<sup>18</sup>

If you accept that black is "something," then Ostwald's proposition<sup>19</sup> that any color is made up of a "full color" (Ostwald proved to his satisfaction that full colors are semichromes), some white and some black makes good sense. That works fine in the Ostwald description and it works fine with the RGB description.

The HWB of Alvey Ray Smith (if only he had made it HWK, for "B" is already used for blue!) is the implementation of Ostwald's ideas in RGB, although Smith didn't notice.<sup>20</sup> It is by a wide margin the most "natural" description. Smith even called other RGB descriptions flawed, although — as an early engineer in image processing and computer graphics — he had defined a few of these (HSV, HSL, still in common use) himself.

Figure S17 compares the various choices. Take your pick.

<sup>17</sup> See:

H. von Helmholtz (1867). Handbuch der physiologischen Optik. Voss, Hamburg und Leipzig.

E.Hering (1905–1911), Grundzüge der Lehre vom Lichtsinn. Sonderabdr. a. d. Hdb. d. Augenheilkunde. Voss, Leipzig.

<sup>&</sup>lt;sup>18</sup> J.W.Goethe (1810) Zur Farbenlehre. Tübingen: Cotta.

<sup>&</sup>lt;sup>19</sup> W.Ostwald (1917). Die Farbenfibel. Unesma, Leipzig.

<sup>&</sup>lt;sup>20</sup> A.Smith and E.Lyons(1996). *HWB — A more intuitive hue-based color model.* Journal of graphics, gpu, and game tools 1(1), 3–17.

### 8 OSTWALD MISMATCHES

As discussed in the manuscript, Ostwald's intuition (fig. S18) is a fine heuristic, but deviates from the actual colorimetric structure. The deviations are noticeable in fig. S19, the mismatch angle  $\xi$ , indicated in ??, has been plotted in fig. S20. We discuss some of the relevant geometry.

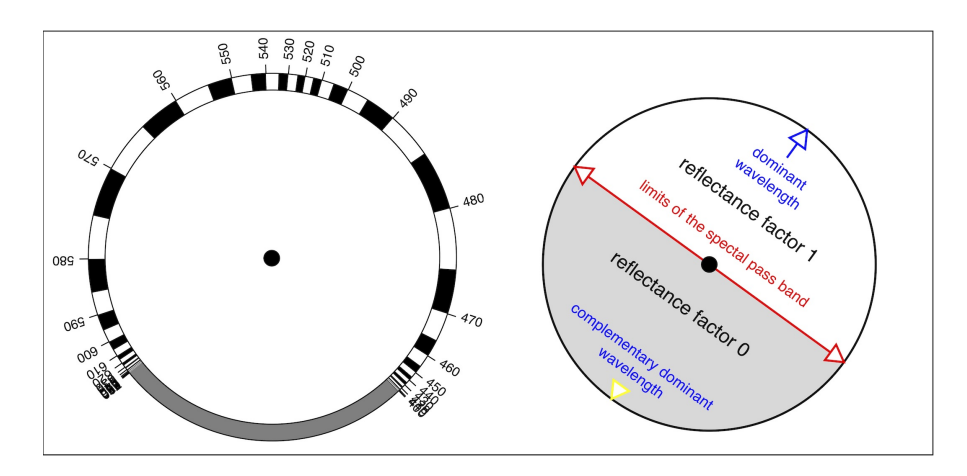


Figure S18. These are the two sheets of Ostwald's "slide rule."

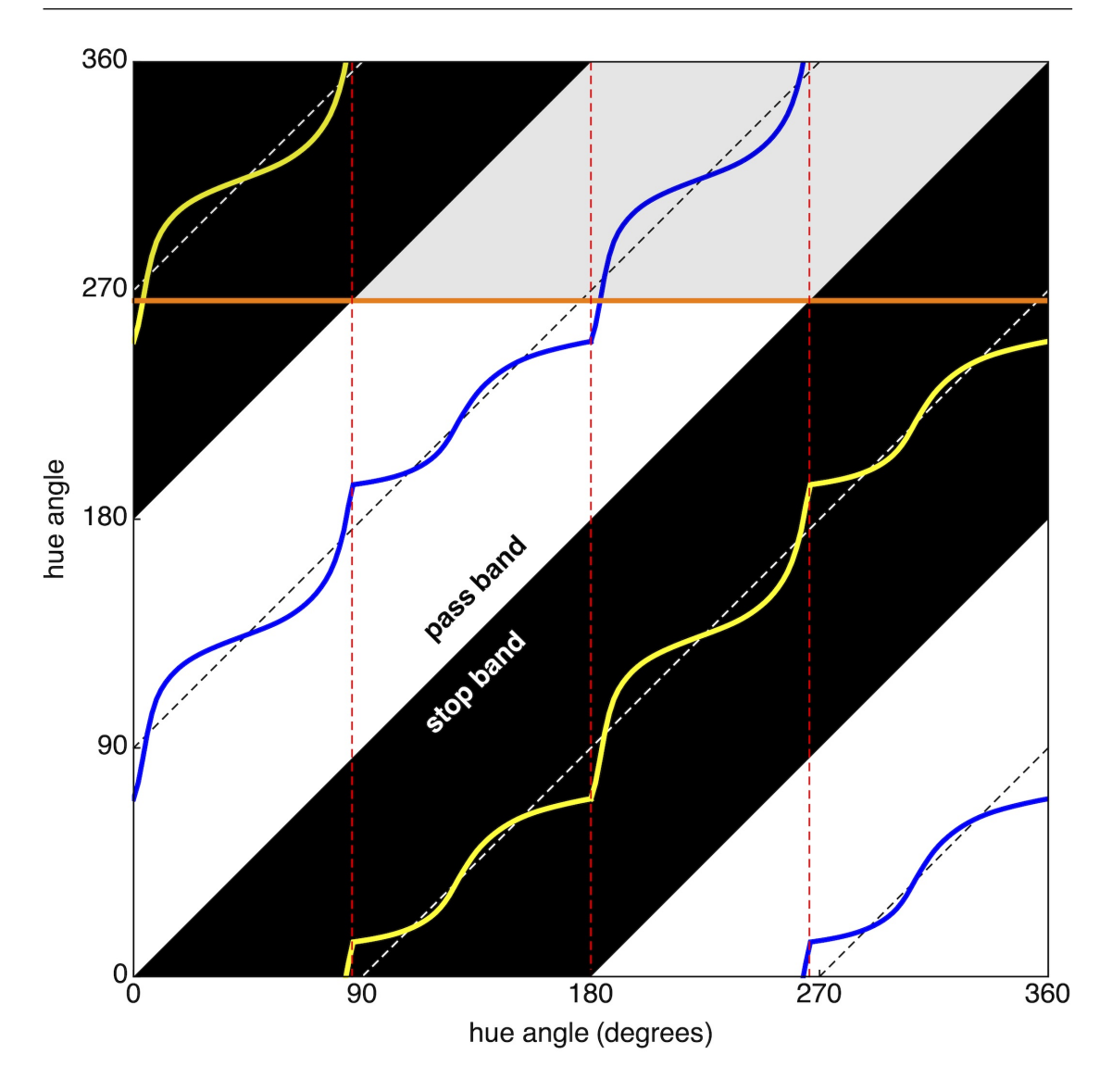
Consider fig. S20 top-left. Here A is the achromatic point and B a semichrome. This implies that the diagonal is parallel to the tangent t at the semichrome locus. The semichrome B is given by (using the notation used in the article)

$$B = \int_{\lambda_1}^{\lambda_2} \mathbf{M} \, \mathbf{R}(\lambda) \mathcal{E}(\lambda) \, \mathrm{d}\lambda = \int_{\lambda_1}^{\lambda_2} C(\lambda) \, \mathrm{d}\lambda, \tag{S3}$$

Where  $C(\lambda) d\lambda$  is a "monochromatic color," and  $\lambda_{1,2}$  are mutually complementary. Note that  $\delta B = C' \delta \lambda_2 - C \delta \lambda_1$ , where  $\delta \lambda_{1,2}$  are arbitrary variations. Because  $C\delta \lambda_1$  and  $C'\delta \lambda_2$  are mutually complementary,  $\delta B$  lies in the plane spanned by the achromatic axis and the diagonal CC'. This proves that indeed  $CC' \parallel t$  (fig. S20).

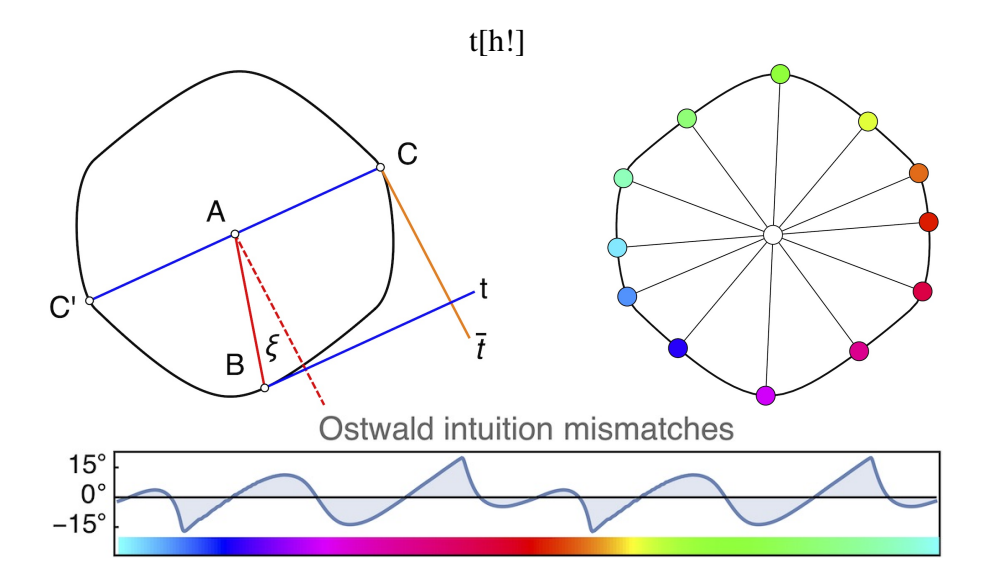
If the semichrome locus were an ellipse (which it is evidently not!), the tangent t' at C would be parallel to AB (so called "conjugate diameters" of an ellipse). If the semichrome locus were a circle (which again, it is evidently not!), the tangent t' at C would be  $\|AB\|$  and AC. This is were Ostwald went wrong as he habitually thought of the semichrome locus as the COLOR CIRCLE (as in fig. S18). The BAC and the intersection tt' would be a square. As evident from fig. S20 it is a general quadrangle instead.

However, Ostwald's intuition was not completely off, the interquartile range of the mismatch is  $\pm 8.6^{\circ}$ , deviations less than ten percent from the "ideal"  $90^{\circ}$  angle subtended

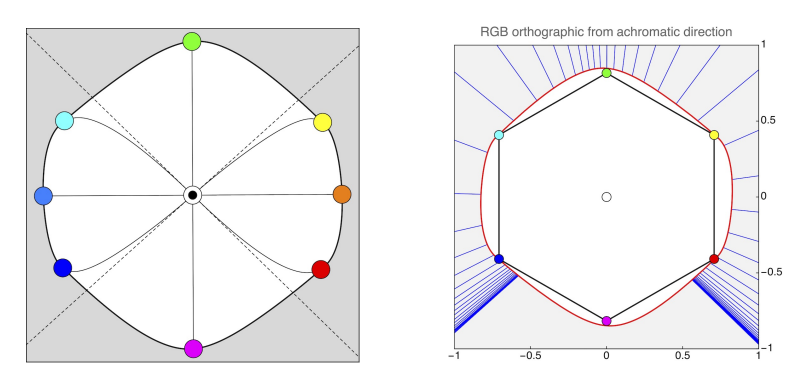


**Figure S19.** In this "Ostwald diagram" Ostwald's intuition covers only the dashed diagonal lines. The domain is the product of the color circle with itself, that is  $\mathbb{S}^1 \times \mathbb{S}^1 = \mathbb{T}^2$ , the torus. Thus the diagram is doubly–periodic. At top we shade an extra-spectral part. A precise computation of the full colors reveals that the oblique dashed lines suggested by the heuristic are actually intricate curves (blue dominant wavelengths, yellow complementary dominant wavelengths). The original intuition remains an excellent approximation.

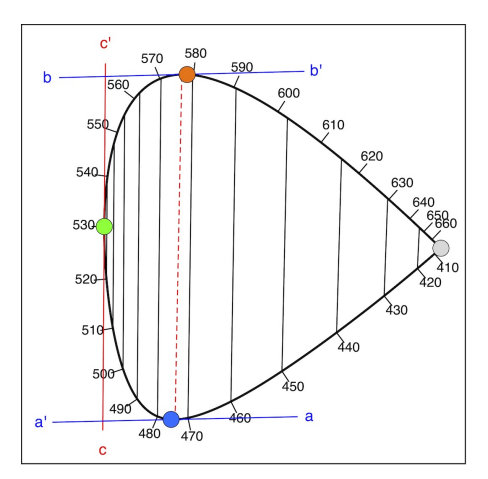
by AB and t. It would have been nice if the semichrome locus had been circular, but it isn't. Biological evolution only does effective hacks, this one is apparently "good enough."



**Figure S20.** Ostwaldian mismatches. The rounded hexagon is the semichrome locus in the chromaticity diagram. At top-left the basic geometry: B is semichrome, thus the tangent t is parallel to the diagonal CC', but the tangent t' at C is not parallel to AB, except for some remarkable locations. At top-right the semichromes for which the mismatch vanishes. At bottom a plot of the mismatches. They start to be of significance for a color circle of 24-steps, but are irrelevant in generic applications.



**Figure S21.** This "chromaticity diagram" is an orthogonal view from the achromatic direction. For object colors, it is far more useful and intuitive than the familiar CIE conventions. This shows the achromatic axis (central point, both white and black), the semichrome locus (in this projection the outline of the color solid), the edge–colors (figure–eight curve), the limiting spectrum generators and their complementaries (thus indicating the types of Ostwald full color families) and the cardinal color locations. It also shows the mutually orthogonal Hering directions, green–purple and teal–orange. This offers a convenient canvas to plot all kinds of things in an intuitive context. (fig. S22 and ??.) In the figure at right we added the spectrum cone generators (in the exterior) and the RGB–cube (the hexagon).



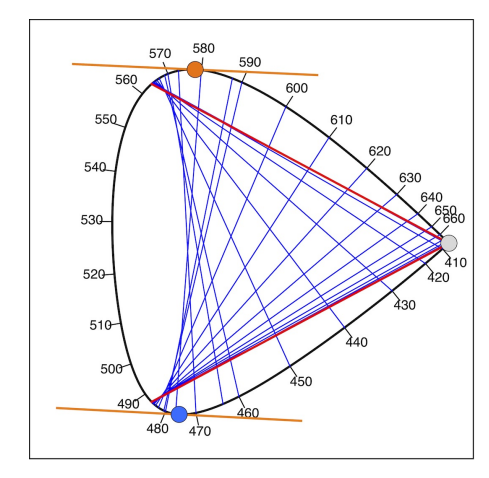


**Figure S22.** This illustrates how the cool edge color curve in the chromaticity diagram (fig. S21) can be used to find interesting relations. Notice that aa' and bb' are mutually parallel, thus the dashed red line is the semichrome chord. All other parallel chords are shorter and indicate tints and shades of the same dominant wavelength. The chord of zero length is the tangent cc' and indicates the dominant wavelength of the semichrome. In the figure at right all blue chords have parallel tangents at their ends (one example shown). Thus they all indicate semichromes. The red lines indicate the complementaries of the spectrum limits.

In fig. S21 we show the "chromaticity diagram" with the semichrome locus (the outline, the semichome locus is the "equator of the color solid) and the boundary color loci. This is a very useful structure. The figure shows how you can do interesting (certainly not trivial) computations graphically. Once you understand such constructions, you significantly honed your intuitive understanding of object colors.

Figures S22 and S23 take this a step further. Figure S23 also illustrates the origin of Ostwald's error.

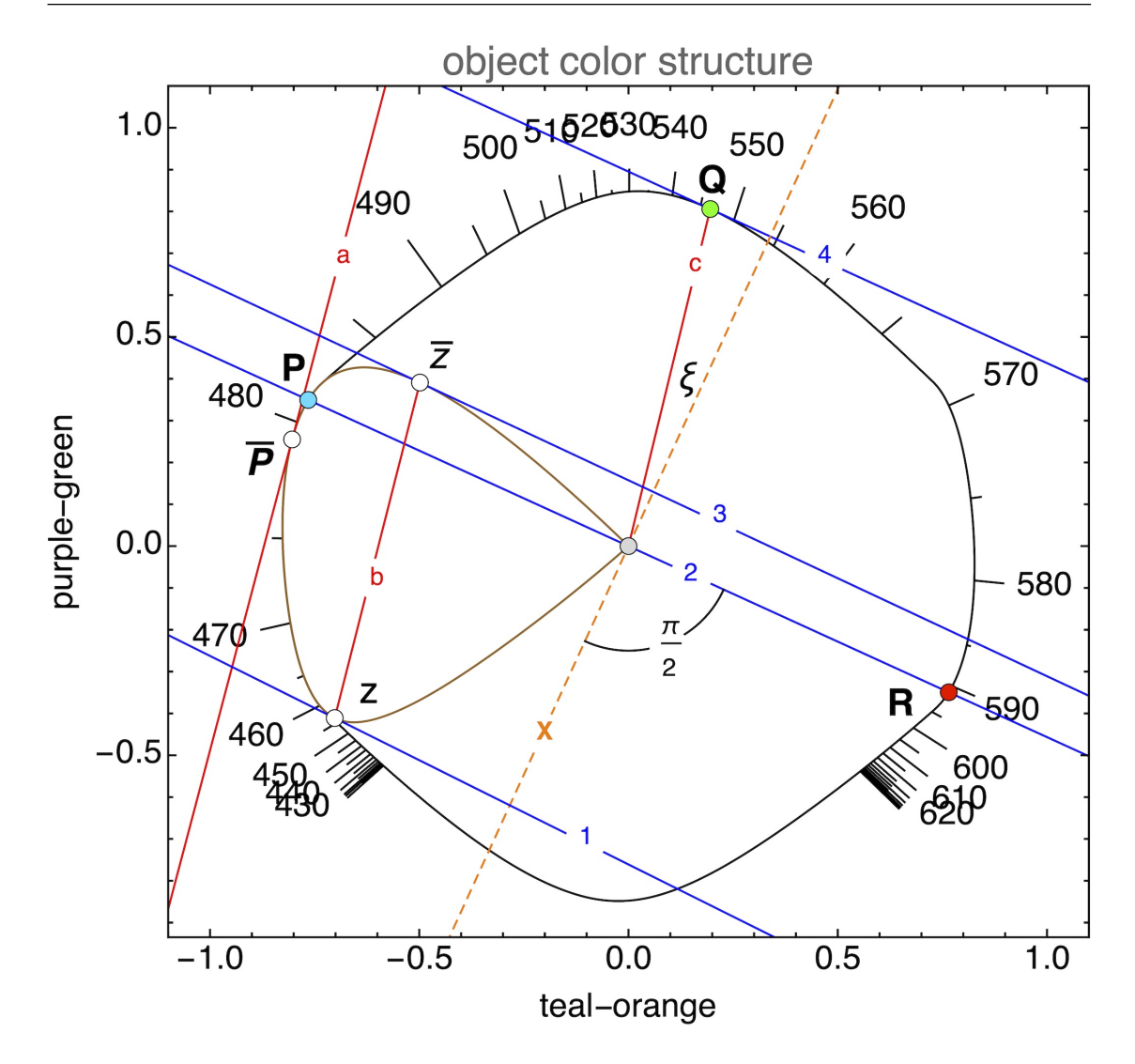


**Figure S23.** This shows even more structure than fig. S22. All red lines (a, b, c) are mutually parallel, so are the blue (1, 2, 3, 4) ones. The dashed orange line (marked "X") is drawn perpendicular to the blue ones. Note the angle  $\xi$  subtended with the red lines. This is the quantitative error of Ostwald's slide rule. Note also that **P** is on the semichrome locus, whereas  $\overline{P}$  (as z and  $\overline{z}$ ) is on the edge–color curve. (The blue tangent 3 is at  $\overline{z}$ .) **Q** is the semichrome color, whereas **P**, **R** are the pass band limits. (In the figure the dominant wavelength of the semichrome is 546.5nm (**Q**), the band limits are 481nm (**P**) and 591nm (**R**).) This illustrates the meaning of the chromaticity diagram (fig. S21). The reader may want to construct such diagrams for the other semichrome families. (Note: in typical applications your construction will commence from the point **Q**.)

## 9 AN OSTWALD BASIS AND THE RGB BASIS

The Ostwald system uses an over-complete, continuous basis (fig. S24). The mixtures of the achromatic colors with the semichromes span a double cone.<sup>21</sup> The double cone exhausts 78.5% of the color solid, so it does better than the RGB cube (64%). However, the double cone and the RGB cube strongly overlap, the Jaccard index is 0.80. A comparison of the color solid, the Ostwald double cone and the RGB cube reveals their overall similarity (fig. S25).

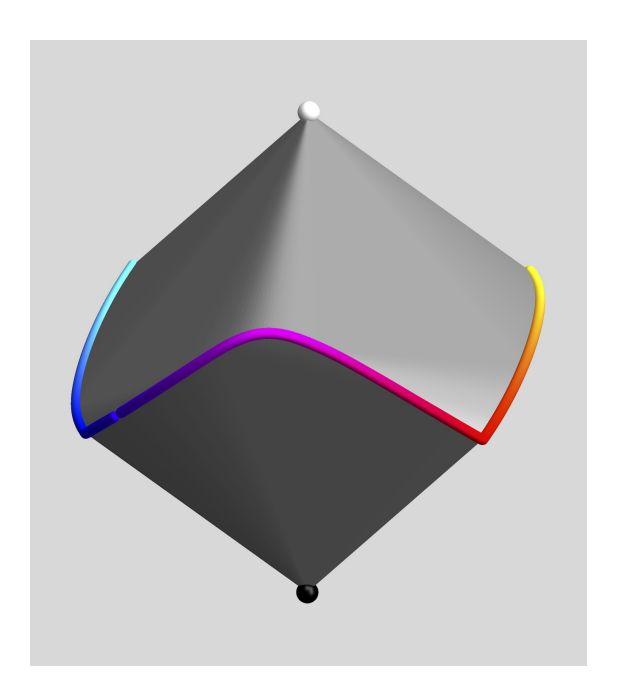


**Figure S24.** The Ostwald double cone as it should have been. Ostwald used a circle instead of the semichrome locus.

Thus the Ostwald basis is really different from the tripartite (optimal basis). In trying to compare one might try to set up a minimal (three basis vectors) basis of semichromes.

The green vector of the tripartite basis is an optimal color with a passband that is slightly narrower than a semichrome. The difference is small though. One might accept the semichrome with the same dominant wavelength as the tripartite green for an Ostwald-type basis vector.

As a suitable red vector the semichrome with pass band  $\overline{\lambda}_{UV} - \lambda_{IR}$  is an obvious, unique candidate. As a suitable blue vector the semichrome with pass band  $\lambda_{UV} - \overline{\lambda}_{IR}$  is the obvious choice.

<sup>21</sup> Ostwald did not use this construction, he used a circle instead of the semichrome locus. This looks good, but is formally awkward.

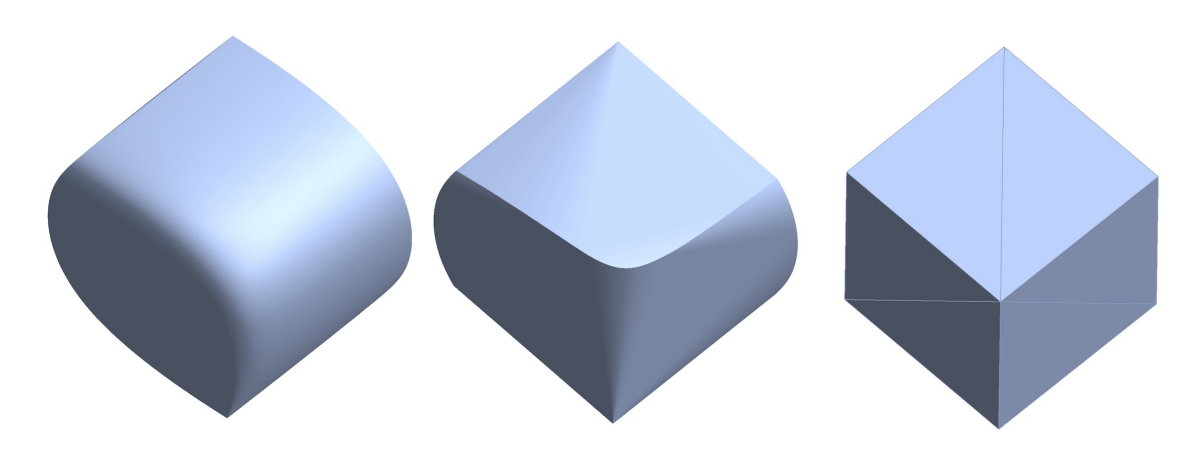


**Figure S25.** A comparison of the color solid, the Ostwald double cone and the RGB cube, plotted at the same scale. The overall similarity is striking.

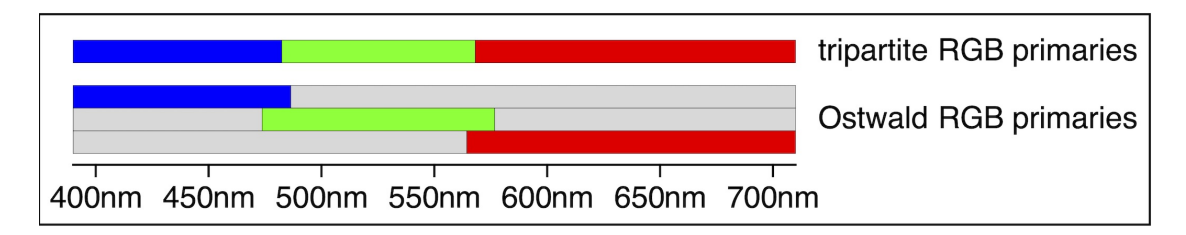


**Figure S26.** Ostwald uses a continuous basis, instead of a discrete (*e.g.*, RGB basis). It is easily possible to define three "special" full colors that represent red, green and blue though. However, they do not form a true spectrum tripartition, since their passbands overlap. Although the Ostwald system is elegant it is very hard to implement. In fact, we do not know a single useful instance. In practice, most of Ostwald's (valuable!) notions work just as well in the RGB basis.

This set of vectors defines a basis (not actually used by Ostwald) that is very similar to the tripartite basis, but fails to be orthonormal. However, the matrix of pairwise dot-products is not that far from  $I_3$ . This basis is somewhat different from the tripartite basis (fig. S26). It apparently is less than elegant to use an non-orthonormal basis, moreover this Ostwald crate (not his double—cone!) captures a (only very slightly) smaller gamut than the RGB basis does. Plenty of reasons to prefer RGB in practice, although the Ostwald formalism is nice enough.

The Ostwald full colors lie exactly on the semichrome locus because they are semichromes. The RGB full colors (cardinal colors) can in general not be semichromes, because the only possible transition loci are fixed and not mutually complementary. As expected, green and magenta do not lie on the semichrome locus, whereas the other cardinal colors do. Note the difference between the Ostwald and the RGB basis vectors (fig. S27).

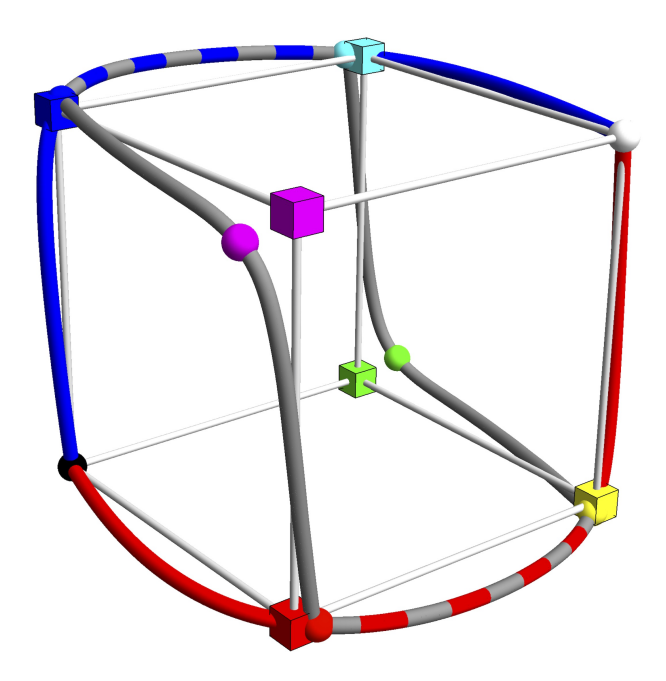


**Figure S27.** The RGB (colored cuboids) and Ostwald locations (colored spheres) of the cardinal colors in relation to the semichrome locus (gray). The cool boundary colors are drawn in blue, the warm boundary colors in red. Over some stretches the boundary color loci coincide with the semichrome locus. The relation to the RGB cube (light gray, thinnish) is very close. The deviations between the RGB and the Ostwald primaries are most noticeable in the green and purple.

The continuous Ostwald basis is unwieldy, both formally and in implementation (say display units). Pragmatically, it was convenient for Ostwald's chemical applications. It is next to impossible in printing or electronic display technologies.

Another continuous basis is the set of all optimal colors. It captures the maximum gamut, the full color solid. A natural canonical spectral reflectance is the linear mixture (of the spectra, not the colors!) of the optimal color collinear with the center of the color solid, where the spectrum of the centre is taken as flat. In principle such a system is impossible to beat, in practice its implementation would be a nightmare.

Despite that the Ostwald heuristic is quite useful, it has been largely ignored in recent times (fig. S28). It was widely used in continental Europe (including Russia) before WW–II, after that largely ignored. Reference points are Ostwalds *Farbenfibel* of 1916, its translation into English *The Colour Primer* of 1930, Bouma's *Kleuren en kleurenindrukken* of 1946 (translations into English, French and Spanish soon after) and the standard text on colorimetry by Wyszecki and Stiles *Color Science* of 1960.

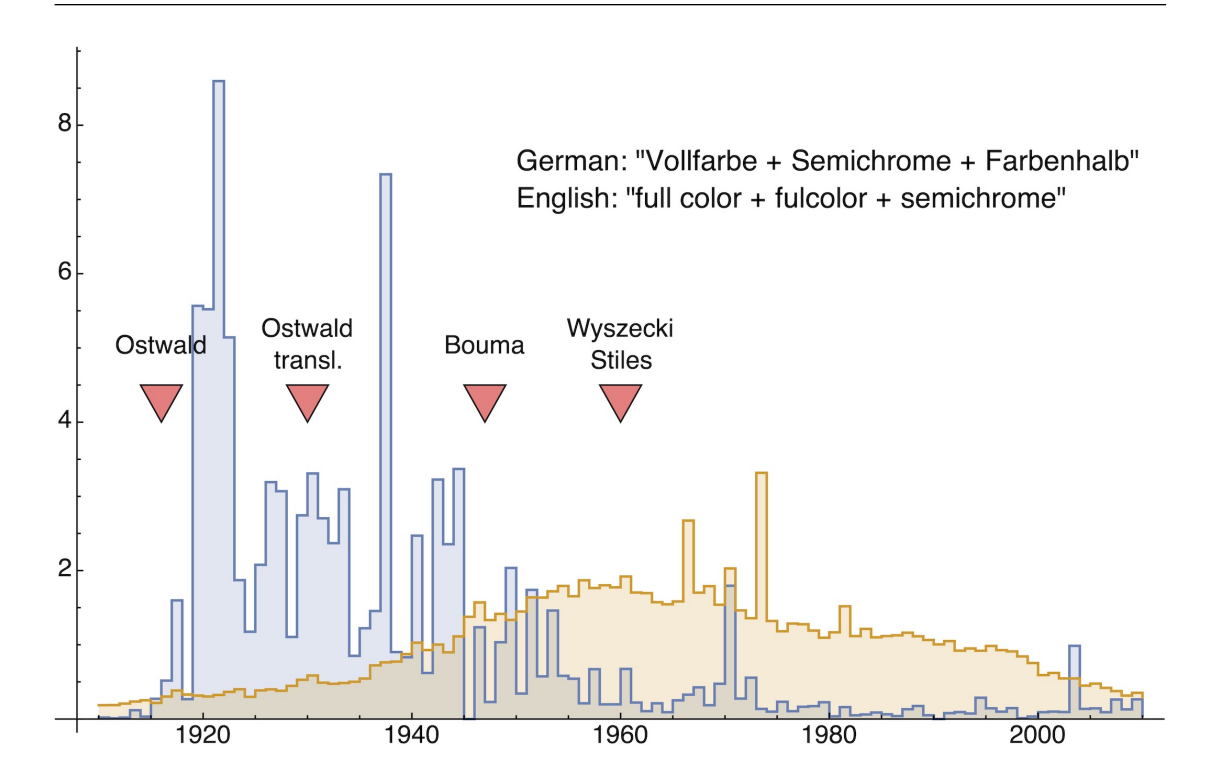


**Figure S28.** The occurrences of Ostwald's terms over a century (1910–2010) in the German and English literature. We use Google n-grams search for the indicated search terms. Abundancies have been normalized on the mean. No matter how you look at it, the end of the Ostwald description is in the decade after WW–II. From then CIE XYZ takes over, in the 1990's followed by CIE Lab.

## 10 MINIMAX AND MAXIMUM ENTROPY HEXAPARTITION SPECTRA

Given an object color, is there a "best" hexapartitive reflection spectrum (section 14)? Since there is no unique solution, one needs a constraint. Suitable candidates might be maximum entropy solutions or "minimax" ones. We found the latter generally somewhat superior.

Suppose the color is C. Let the hexapartition coordinates be  $\{p_1 \dots p_6\}$ , with  $0 \le p_i \le 1$  for  $i = 1 \dots 6$ . Let the six bin colors be  $\{C_1 \dots C_6\}$ . Then the color corresponding to  $C_p = \{p_1 \dots p_6\}$  is  $\sum_{i=1}^6 p_i C_i$ . (Notice that  $p_i = 1$  for  $i = 1 \dots 6$  yields the white color.) We require  $C_p = C$ , and minimize the total variation  $[\max p - \min p]$ .

Thus one obtains a hex spectral reflectance function for any color that is of minimum total variation.

Maximizing  $\sum_{i=1}^{6} (-p_i \log_2 p_i)$  yields maximum entropy solutions. This works quite well too. In the article we stick to the minimax solutions for the sake of simplicity.

The hex spectra are "canonical spectra" of some kind, they are only metamers of the actual spectra that caused the color. In experiments on databases of ecologically valid spectral reflectance factors, we find that both methods tend to yield very good approximations to the actual spectra. The reason is — no doubt — that actual spectra tend to be quite smooth.

## 11 THE BLACK BODY FAMILY OF SOURCES

For a thermal radiator in thermodynamic equilibrium Planck showed that the spectral radiance (using SI units in W·sr<sup>-1</sup>·m<sup>-3</sup>) on wavelength basis is a function  $B(\lambda, T)$ , which depends on the physical constants c, velocity of light, h, Plank's constant, and  $k_B$ , Boltzmann's constant.<sup>22</sup>

$$B(\lambda, T) = \frac{2hc^2}{\lambda^5} \frac{1}{e^{\frac{hc}{\lambda k_B T}} - 1}.$$
 (S4)

As a function of wavelength the radiance has a single peak at  $\lambda_{peak} = b/T$ , where  $b = 2.8978 \cdots 10^{-3} \text{m·K}$ . The peak is at the centre of the visual range (525nm) for  $T = 5520^{\circ}\text{K}$ . The spectrum is almost an equi-energy spectrum (deviations less than  $\pm 10\%$ ). For  $T = 4081^{\circ}\text{K}$  the peak is in the UV, for  $T = 7430^{\circ}\text{K}$  it is in the IR.

Reckoning radiance with respect to the  $T=5520^{\circ}\mathrm{K}$  case, one has

$$B_{rel}(\lambda, T) = c_1 \lambda^{-5} (e^{\frac{c_2}{\lambda T}} - 1)^{-1},$$
 (S5)

with  $c_1=5.6764\,10^{15},\,c_2=1.4388\,10^7,\,$  where T is in degrees Kelvin and  $\lambda$  in nanometers. Thus  $B_{rel}(525,5520)=1,\,$  whereas  $B_{rel}(525,T)\propto T^4$  (the Stefan–Boltzmann Law). This is the most convenient form for vision–related problems. (Figure S29.)

<sup>&</sup>lt;sup>22</sup> R.Feynman, R.Leighton and M.Sands(1964, 1966). *The Feynman Lectures on Physics*. Library of Congress Catalog Card No. 63-20717, Washington DC.

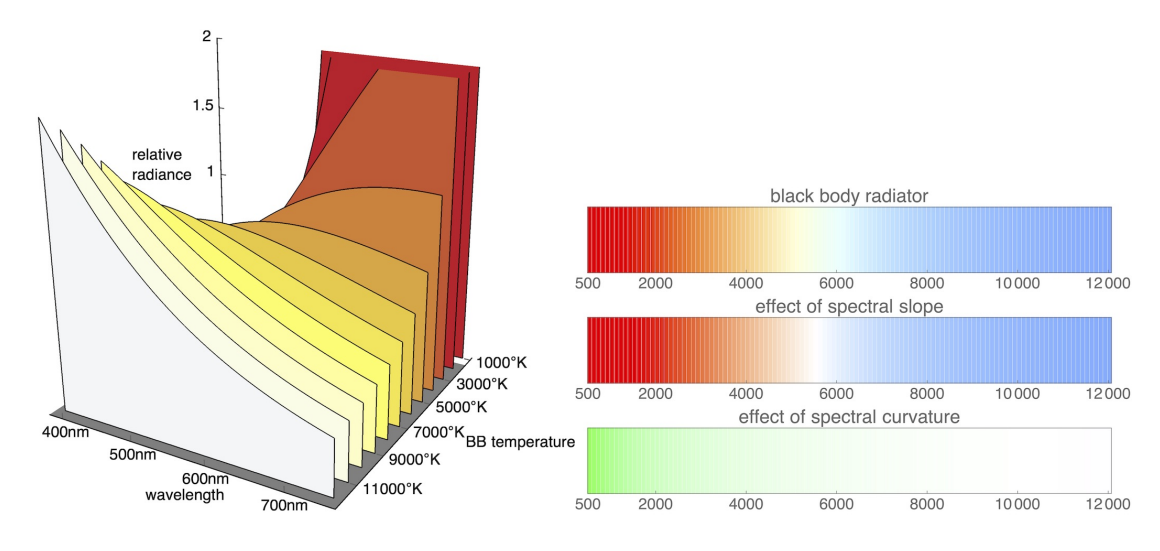


**Figure S29.** At left black body radiant power spectra, normalized to one at 530nm. At top-right the color of a white standard in the absence of AWB ("automatic white balance"). We also show the influence of spectral slope and curvature individually.

In order to get the magnitudes in context, the sun's photosphere radiates at  $5777^{\circ}$  K, the blue sky has a "correlated color temperature" of up to  $12\,000^{\circ}$  K, whereas a tungsten bulb (a thermal radiator) radiates at  $3400^{\circ}$  K and an ancient Roman oil lamp burning animal fat below  $1000^{\circ}$  K. This covers about the range encountered in real life. Roughly speaking, candle light has a negative spectral slope, sky light a positive spectral slope, normal daylight is not too far from the equal energy spectrum. Human vision needs to deal with all of these.

The black body radiator family is very convenient because it is ecologically relevant and well defined. Although only a one-parameter family, the fact is that — give or take a little slop — this pretty much exhausts the range of ecologically important sources. Fancy Las Vegas bars are exceptions, they are based on rare earth (especially lanthanides) atomic electronic structures.

## 11.1 A two-parameter set of radiant spectra

The black body family varies mainly along the spectral slope dimension. It does a good job of catching the major variation, but it fails to cover the range. This is a reason for kludges like "correlated color temperature" and so forth.<sup>23</sup> For a generic set of sources

<sup>&</sup>lt;sup>23</sup> G.Wyszecki and W.S.Stiles (1967). Color science: Concepts and methods, quantitative data and formulae. Wiley, New York.

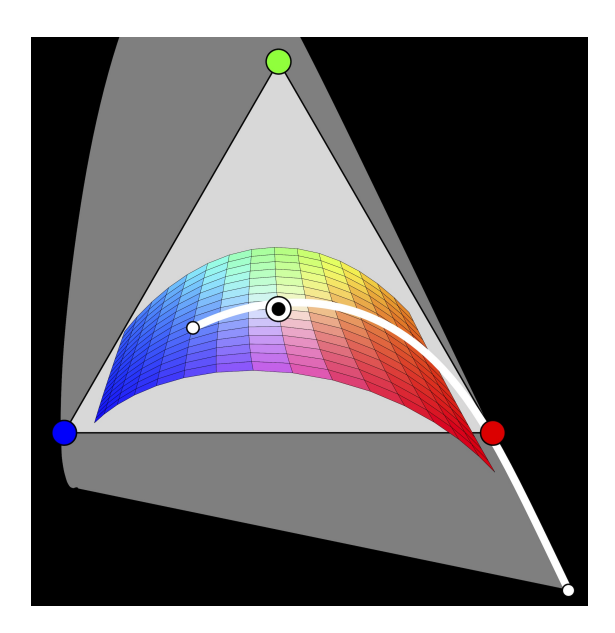


**Figure S30.** Spectral slope and curvature eq. (S6) in the RGB chromaticity diagram. This diagram is similar to the CIE-xy-diagram, but the RGB primaries lie on an equilateral triangle. It is often called "Maxwell triangle," despite the fact that Maxwell himself calls it the "Mayer triangle" (after Tobias Mayer, 1723–1762). The white curve is the Planckean locus.

one needs to include spectral curvature. This adds another parameter and thus covers a two-parameter range of chromaticities. More general sources then simply differ by metameric black spectra, so the choice is non-committal.

Since radiance is a non-negative quantity, its natural domain is logarithmic. Thus one defines a generic family of source spectra as (s the slope, c the curvature)

$$S_{s,c}(\lambda) = e^{s\left(\frac{\lambda - \lambda_0}{\Delta \lambda}\right) + \frac{1}{2}c\left(\frac{\lambda - \lambda_0}{\Delta \lambda}\right)^2},$$
(S6)

with  $\lambda_0 = 525$ nm,  $\Delta \lambda = 100$ nm (say). The set of black body spectra is captured quite well (so little new here), but there is a second degree of freedom (fig. S30).

## 11.2 Random daylight spectra

In order to generate "random daylight spectra,"<sup>24</sup> one might use the two-parameter radiant spectra defined in the previous sub-section, and add a contribution due to the scattering from the immediate environment. These latter spectra can be based on some statistical model for generic spectral reflectance factors.

One needs to draw the two parameters from a distribution that may be estimated from a database of daylight spectra obtained from a large range of conditions. Using a two parameter normal distribution, one requires two means and a covariance matrix. However, the overall intensity is irrelevant, thus there are four degrees of freedom. The fraction of ambient scattering yields another degree of freedom, as do the degrees of freedom in the model of spectral reflectance factors.

Such random daylight generators are essential in the numerical study of the effects of metamerism. One would certainly like to have ecological statistics on the parameters. Unfortunately, such are hardly forthcoming. In practice one has to make do with "intelligent" guestimates.

<sup>24</sup> See:

J.J.Koenderink, A.J. van Doorn and K.Gegenfurtner (2020). Colors and things. i-Perception 11(5), 1–43. and

J.J.Koenderink and A.J.van Doorn (2020). Orange & Teal. Art & Perception, in press.

#### 12 RANDOM REFLECTANCE SPECTRA

When one studies databases of natural spectral reflectance factors or even RGB colors (images are a great source), one finds that spectral reflectance factors are comparatively "smooth" and that gamuts of pixels fail to fill the RGB cube homogeneously.<sup>25</sup>

For a typical image of a natural scene, the correlation matrix for the RGB-coordinates will be close to

$$\mathbf{h} = \begin{pmatrix} 1 & 1 - \xi & 1 - \eta \\ 1 - \xi & 1 & 1 - \xi \\ 1 - \eta & 1 - \xi & 1 \end{pmatrix}, \tag{S7}$$

where  $0 < \xi \ll 1$ ,  $0 < \eta \ll 1$ . In many cases one finds  $\eta \approx 2\xi$ , we will use that here for the sake of simplicity. The eigenvectors are approximately  $\{1,1,1\}$ ,  $\{1,0,-1\}$  and  $\{-1,2,-1\}$ , that is the Hering basis.

The key point is the ecological fact that spectral reflection functions tend to be smooth. That implies that they will be well approximated by level, slope and curvature. That is indeed found in studies that consider principal components of the spectral reflectance functions.<sup>26</sup>. This fact is also useful in attempts to discount the illuminant.<sup>27</sup>

Apparently the Hering basis serves to decorrelate the RGB channels. Indeed, the first Hering vector estimates the spectral level, the second the spectral slope, and the third the spectral curvature. The Hering color matching functions are like a set of receptive fields<sup>28</sup> acting on the spectral envelope.

The ratio of eigenvalues are  $1: 2\xi/3, 2\xi/9$ . Thus the black-white dimension by far dominates whereas the teal-orange dimension has thrice the power of the purple-green dimension. For a typical value  $\xi \approx 0.1$  the ratios are 1:0.067:0.022.

This implies that the envelope of the spectral reflectance factors has a correlation length of more than the width of the visual spectrum. Almost all of the power is in the level, much less in the slope, and even less than that in the curvature.

<sup>&</sup>lt;sup>25</sup> See:

J.J.Koenderink, A.J. van Doorn and K.Gegenfurtner (2020). Colors and things. i-Perception 11(5), 1–43.

J.J.Koenderink and A.J.van Doorn (2017). Colors of the sublunar. i-Perception, 8(5).

<sup>&</sup>lt;sup>26</sup> As for instance Vrhel, M.J., Gershon, R. and Iwan, L.S. (1994) "Measurement and analysis of object reflectance spectra". Color Research and Applications, 19, 4–9; Maloney, L. (1999). Physics-based approaches to modeling surface color perception. In K.R. Gegenfurtner, and L. T. Sharpe (Eds.), Color vision: From genes to perception (pp. 387–422). Cambridge University Press.

<sup>&</sup>lt;sup>27</sup> As for instance B. Singh, W. Freeman, and D. Brainard (2003), "Exploiting spatial and spectral image regularities for color constancy," in Proc. 3rd Int'l Workshop on Statis. Comp. Theories of Vision, Nice France, 2003; S. Jimenez and J. Malo (2014), "The Role of Spatial Information in Disentangling the Irradiance–Reflectance–Transmittance Ambiguity," IEEE Trans. Geosci. Rem. Sens., vol. 52, no. 8, pp. 4881–4894

<sup>&</sup>lt;sup>28</sup> J.J.Koenderink and A.J.van Doorn (1990). Receptive field families. Biol. Cybern. 6, 26, 291–297.

This has major implications for the RGB gamuts to expect. For instance, consider one of the simplest conceptual models, which might be a random telegraph wave toggling between all or none reflectance.<sup>29</sup> There is just one parameter, which is the expected number of transitions within the visual range. For the statistics of the transitions we assume a renewal process, say an exponential distribution. Then what gives? There are four qualitatively different regimes, depending on the expected number of transitions N:

- $N\ll 1$  if the number of transitions is very low almost any instance will be zero or one with fifty-fifty change. Thus one has either black or white colors, chromatic colors will be very rare;
- $N \approx 1\,$  if the number of transitions equals one, one has either a warm or a cool edge color, with fifty-fifty chance. Thus the edge color loci will be populated, but hardly anything else. That implies that the colors will be teals and oranges, there will be no purples and greens;
- $N \approx 2$  if there are two transitions one has an optimal color. Thus the boundary of the color solid will be populated and hardly anything else. Teal, oranges, purples and greens all occur;
- $N\gg 1$  if there are very many transitions the spectrum will almost be a metameric gray. Almost all colors will cluster about the gray point. The diameter of the cluster will depend on the number of transitions, the larger N, the smaller the diameter (easy to estimate by way of a statistical argument).

These predictions are well borne out (figs. S31 and S32). From daily experience one estimates that we are living in a regime  $N \approx 3$ .

The width of the visual range is about 200nm, measures via the edge color curves from 0.1 distance to the black point to 0.1 distance from the white point. If we try  $N=1/10,\,1,\,2,\,20$  we find the correlation matrices

$$\begin{pmatrix} 1 & 0.95 & 0.89 \\ 0.95 & 1 & 0.95 \\ 0.89 & 0.95 & 1 \end{pmatrix}, \begin{pmatrix} 1 & 0.57 & 0.20 \\ 0.57 & 1 & 0.57 \\ 0.20 & 0.57 & 1 \end{pmatrix}, \begin{pmatrix} 1 & 0.38 & 0.00 \\ 0.38 & 1 & 0.38 \\ 0.00 & 0.38 & 1 \end{pmatrix}, \begin{pmatrix} 1 & 0.05 & -0.01 \\ 0.05 & 1 & 0.05 \\ -0.01 & 0.05 & 1 \end{pmatrix}.$$

This is much as expected. The corresponding color gamuts are shown in fig. S31. The distributions in RGB space are shown in fig. S32.

<sup>&</sup>lt;sup>29</sup> J.J.Koenderink (2010b). *The prior statistics of object colors*. JOSA A 27(2), 206–217.

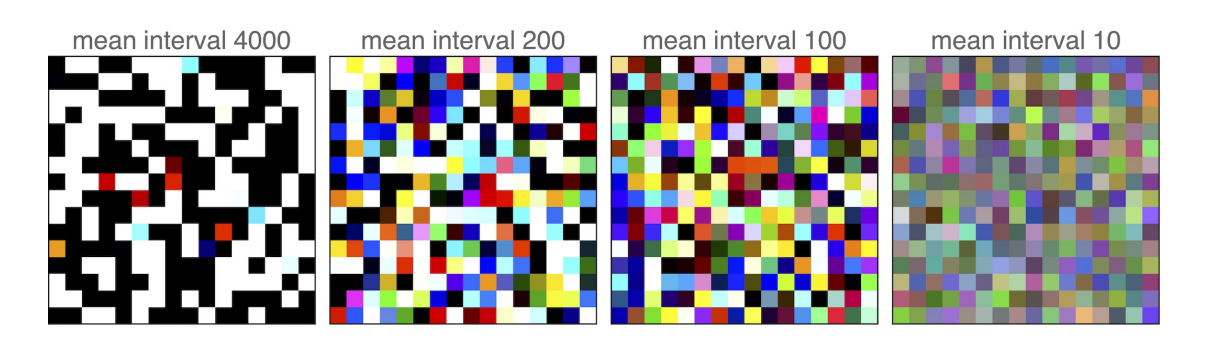
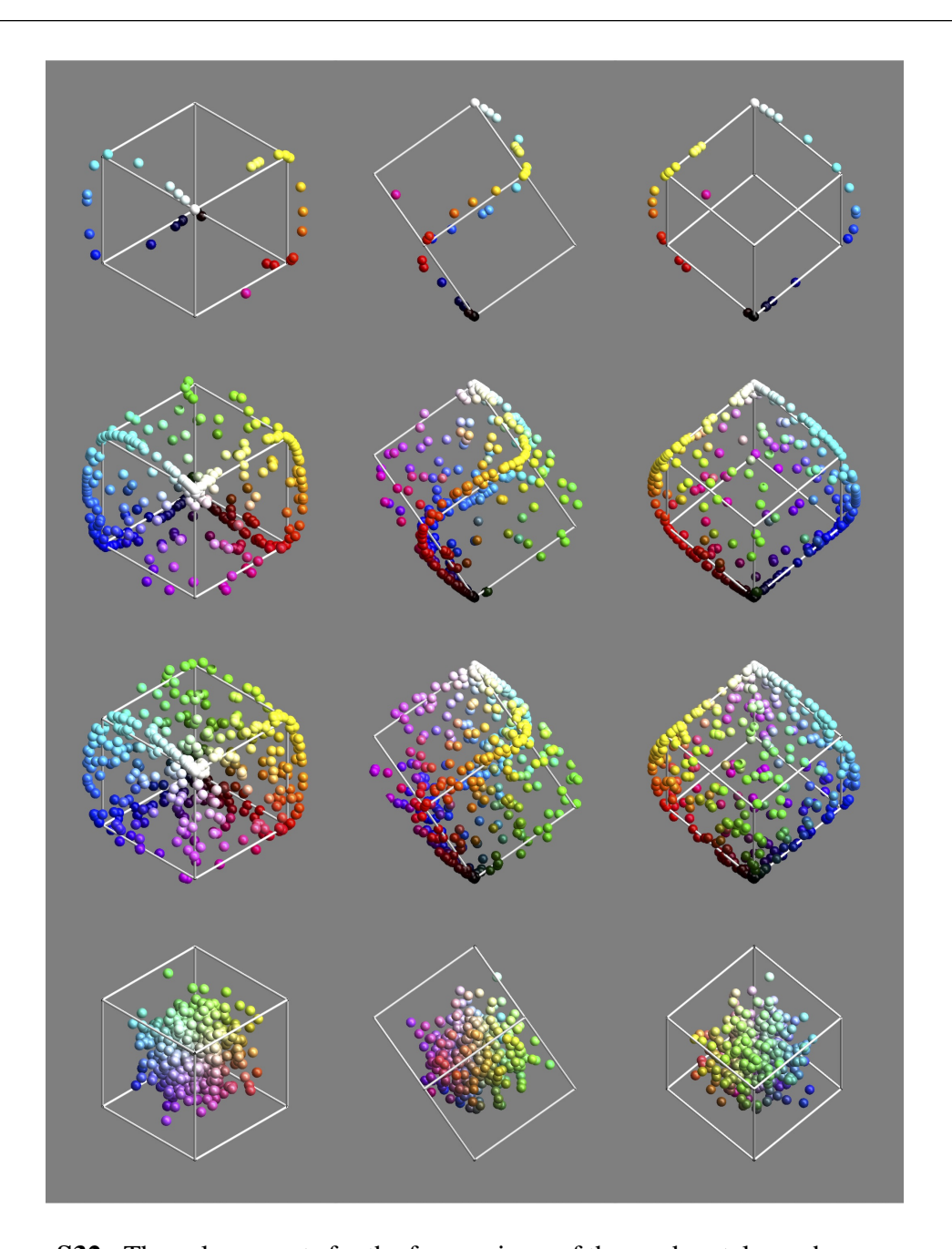


Figure S31. Color gamuts for the random telegraph wave spectra.



**Figure S32.** The color gamuts for the four regimes of the random telegraph wave spectra.

If we study databases of spectral reflectance factors, we find that nearly all show a power spectrum of the spectral envelope that falls off with an exponent of about four.<sup>30</sup> A simple model assumes that the spectral envelope is due to a superposition of random local instances. A suitable model is a Laplace pulse:

$$p(x, x_0, \tau) = \pm \frac{e^{-\frac{|x - x_0|}{\tau}}}{2\tau}$$
 (S9)

where  $x_0$  denotes the location, and where the width at half height is  $2\tau \log 2 \approx 1.386\tau$ . Its Fourier transform is a Cauchy, or Lorenz, distribution. A random superposition of many of such pulses yields a fractal signal with power spectrum

$$S(f,\tau) = \frac{2\sqrt{\frac{2}{\pi}}\tau}{(1+f^2\tau^2)^2}$$
 (S10)

which falls off with the inverse fourth power from the frequency  $f_0 = 1/\tau$ . The corresponding autocorrelation function has a width  $\delta \approx 3.36\tau$ .

Here we have a simple model that allows the generation of random instances.<sup>31</sup>

A problem is that the spectral reflectance factors are only a kind of mirror image of the actual physical domain. In terms of the Kubelka-Munk model<sup>32</sup> one should generate instances of the "spectral signature" and transform that to the unit interval.<sup>33</sup>

Such a simple model readily accounts for the bulk of data bases of spectral reflectance factors. Apparently, with such a simple model of the physics one may abstain from a detailed statistical study of the ecology of the optics of the human life world.

The relative abundance of achromatic, teal—orange and purple—green color families is critically dependent upon the spectral correlation width (fig. S33). This is understood when one studies fig. S34. When the correlation length is much smaller than the visual range one obtains a globular cluster of colors centered on mid gray. All hues (oranges, teals, purples and greens) are about equally present. If the correlation length is much

<sup>30</sup> J.J.Koenderink, A.J. van Doorn and K.Gegenfurtner (2020). *Colors and things. i-*Perception 11(5), 1–43.

<sup>&</sup>lt;sup>31</sup> A numerical method might use the FFT. In this cases one should be wary for artifacts due to the periodicity, as this would boost the purple-greens.

<sup>32</sup> See:

G.Kortüm (1969). Reflectance spectroscopy Principles, methods, applications. Berlin: Springer. and

P.Kubelka and F.Munk (1931). Ein Beitrag zur Optik der Farbanstriche. Zeits. f. Techn. Physik 12, 593–601.

<sup>&</sup>lt;sup>33</sup> See: J.J.Koenderink, A.J. van Doorn and K.Gegenfurtner (2020). *Colors and things. i-*Perception 11(5), 1–43.

J.J.Koenderink and A.J.van Doorn (2017). Colors of the sublunar. i-Perception, 8(5).

larger than the visual range one sees an annular cloud that roughly follows the edge color curves. Thus the colors will be oranges and teals.

This once again reveals the fundamental importance of the Goethian *Kantenspektren*. Goethe's intuitions were to the point, although he could not foresee the reasons, which are due to ecological optics (physics).

This is the final blow to the notion — popular with many philosophers and writers of pop-science — that colors are actually "mental paint" for wavelengths. Monochromatic beams are entirely irrelevant for object colors. The correlation length for articulations of the spectral envelope is perhaps two or more times the width of the visual spectrum.

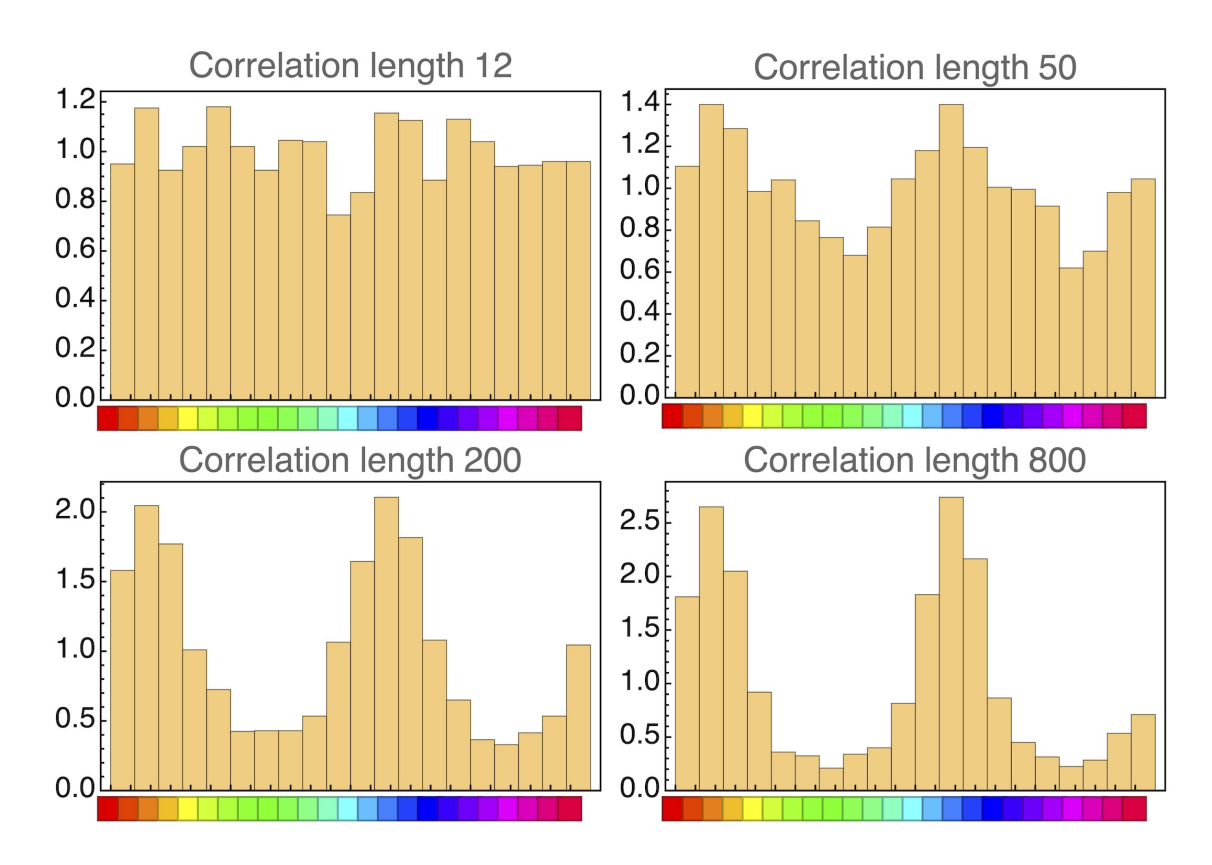


**Figure S33.** The abundancies of hues for various values of the correlation length (stated in nanometers, remember that the with of the visual range is about 200nm). For small correlation length all hue are about equally abundant, but for large correlation length teal—oranges far outnumber the purple-greens. The reason is that the gamut concentrates upon the edge color loci.

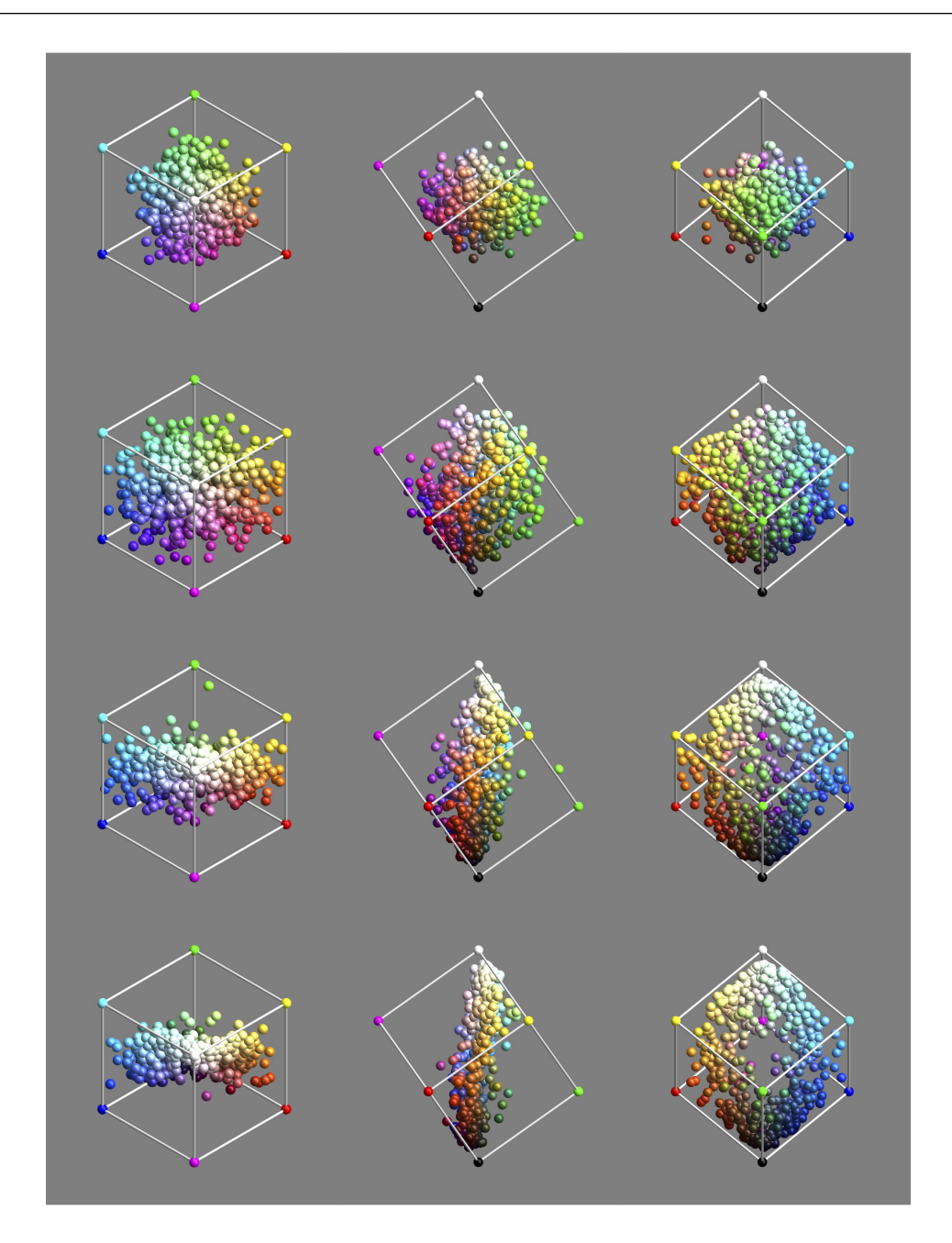


**Figure S34.** The color gamuts for some spectral reflectance factor from a simple model of ecological physics. In the rows from top to bottom the correlation length goes from small to large.

In combination with statistical models of the daylight spectrum one is all set to study the effects of metamerism on RGB colors. This is of great importance for the case of object colors as it largely determines the fuzziness of RGB space. The resulting fuzziness far exceeds the anatomical/physiological graininess as reported by psychophysics. Apparently human color vision in the current state of evolution is largely determined by ecological optics, that is physics.

### 13 CHANGE OF ILLUMINANT

Because of the automatic white balance mechanism, a variation of the illuminant spectrum has only minor influence on the object colors. In the ideal case of *perfect canonical* spectral reflectance factors and *perfect canonical* irradiance spectra there would not be any influence of the source at all, because

$$C = \int_{\lambda_{\text{UV}}}^{\lambda_{\text{IR}}} \mathbf{M} \, \mathbf{R}(\lambda) \mathcal{S}(\lambda) \, d\lambda / \int_{\lambda_{\text{UV}}}^{\lambda_{\text{IR}}} \mathbf{M} \, \mathcal{S}(\lambda) \, d\lambda, \tag{S11}$$

would be independent of the source spectrum  $S(\lambda)$  since equal constant factors in the integrands cancel.

With *actual* spectra it is different, what we will see is due to the effects of metamerism. Fairly extreme cases are shown in figs. S35 and S36. These examples cover about the range relevant to generic human vision. Notice that automatic white balance is evidently not perfect, but is amply good enough for the early hominin hunter-gatherer life style.<sup>34</sup>

In fact, the effects of metamerism are remarkably minor. This may well be a major factor in the evolutionary advantage of having a color vision system as humans actually possess.

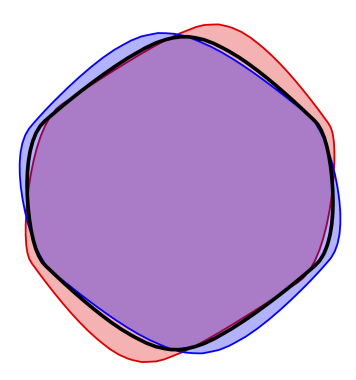


**Figure S35.** AWB renders the orthographic projection of the color solid for very different sources quite similar. The red curve is for  $3000^{\circ}$ K, the blue one for  $12\,000^{\circ}$ K and the black one for the equal-energy spectrum  $\mathcal{E}(\lambda)$ . Note how close these projections are, even for a rather wide range of sources.

The sections through the achromatic axis (fig. S36) reveal small differences for the various hues. The shape of the color solid as a whole is affected. However, it hardly pays

<sup>34</sup> See:

J.J.Koenderink, A.J. van Doorn and K.Gegenfurtner (2020). Colors and things. i-Perception 11(5), 1–43.

J.J.Koenderink, A.J van Doorn and K.Gegenfurtner (2018). Graininess of RGB-Display Space. i-Perception, 9(5), 1-46.

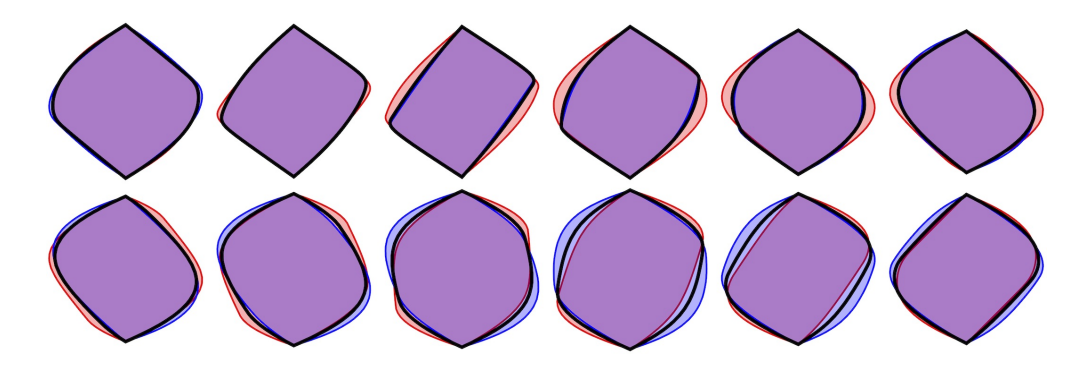


**Figure S36.** AWB renders the color solid for very different sources quite similar. The red curves are for  $3000^{\circ} \mathrm{K}$ , the blue ones for  $12\,000^{\circ} \mathrm{K}$  and the black ones for the  $\mathcal{E}(\lambda)$ –spectrum. Again, note how close the views are for this broad gamut of sources. These are sections through the (here vertical) achromatic axis, a "12 page Ostwald Atlas."

to go into the nitty gritty details. For the hominin it would suffice to use a fairly coarse sampling of the RGB-cube. But even a gamut as small as a few dozen distinct colors would probably be amply sufficient to drive evolution.<sup>35</sup>

<sup>&</sup>lt;sup>35</sup> J.J.Koenderink (2018). *Colour in the Wild*. de Clootcrans Press, Utrecht, the Netherlands.

### 14 METAMERISM

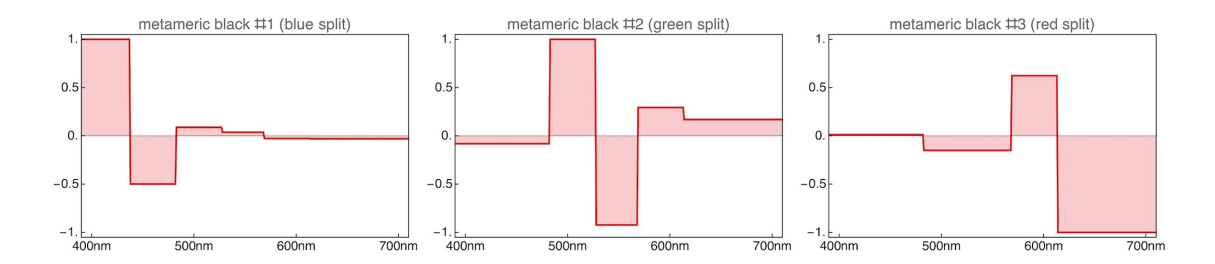
Consider the "hex-basis"

$$\mathbf{h} = \begin{pmatrix} +1 & +1 & 0 & 0 & 0 & 0 \\ 0 & 0 & +1 & +1 & 0 & 0 \\ 0 & 0 & 0 & 0 & +1 & +1 \\ +1 & -1 & 0 & 0 & 0 & 0 \\ 0 & 0 & +1 & -1 & 0 & 0 \\ 0 & 0 & 0 & 0 & +1 & -1 \end{pmatrix}.$$
 (S12)

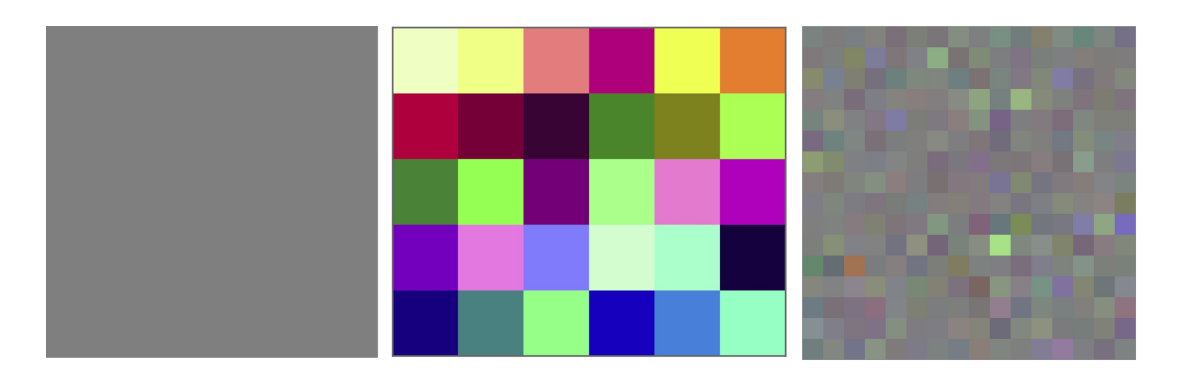
The upper three rows represent the spectrum tripartition, the lower three rows split the three basic components. The cutloci for the split of the RGB parts is done by way of arc-length rectification of the edge—color curves. This refines the tripartition of white into a hexapartition. At least, it is a good start. We proceed by orthogonalization. This does not affect the original tripartition, whereas the lower three rows become a partial basis for the black space (fig. S37). This is arguably the best way to approximate the black space.

Metamers of  $\mathcal{E}(\lambda)$  involve arbitrary amounts of the black components. In a limiting case spectral radiance will fall to zero in at least one of the six parts. Such metameric sources are not revealed by the white standard. Phenomenologically, they all provide  $\sharp$  white light. We prepare twenty-six (all triples of  $\{-1,0,+1\}$ , except  $\{0,0,0\}$ , thus  $3^3-1$ ) of such fake standard sources.

Metamers of the flat central gray reflectance factor, involve arbitrary amounts of the black components. In a limiting case the spectral reflectance will be zero or one in at least one of the six parts. Such metameric reflectance factors are not revealed by the standard source. Phenomenologically, they all are  $\sharp$  central gray. We prepare twenty-six  $(3^3-1)$  of such fake standard gray objects.

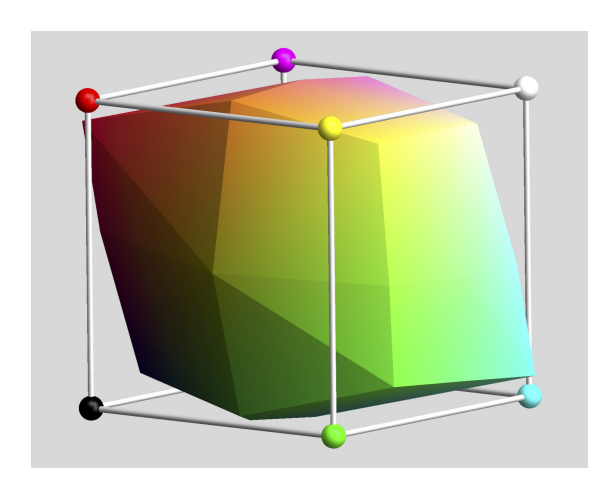


**Figure S37.** These are the "black spectra" used in this section. They are essentially split RGB regions. This set has been orthonormalized.



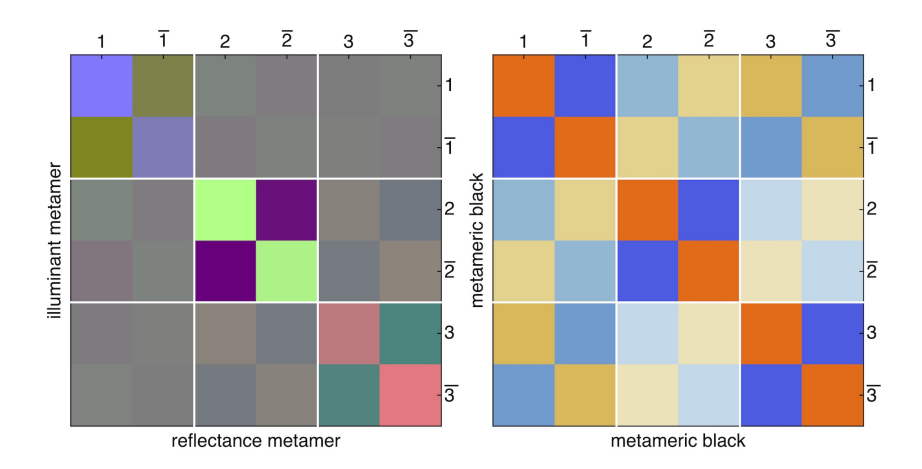
**Figure S38.** Metameric gray colors. This is all about the gray at left under the standard source. The colors at centre are due to spectral reflectances that would look gray under the standard source. Here they are presented under sources under which a truly gray object looks gray. Such sources are not your trusty  $\mathcal{E}(\lambda)$ . The combination of fake "gray objects" and fake "white lights" yields a broad gamut of colors. Any of these might change into any other one at the drop of a hat, if you juggle fake objects and sources. At right the result for "ecologically valid" parameters. Notice the occasional "surprises" due to the marked kurtosis (section 16).

Viewing all fake objects under all fake sources yields  $676~(26^2)$  colors. Only 30 of these lie on the convex hull, which is surprisingly large. It has a volume of 0.83... The vertices of the convex hull are shown in figs. S38 and S39.



**Figure S39.** This is the convex hull of all colors that may be obtained from the hexapartition metamers of the equal energy source and the gray reflectances. It is by no means a minor volume.

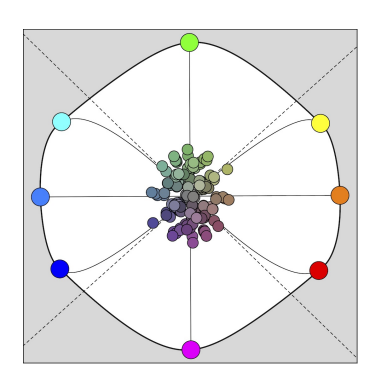
The metameric effects depends on correlation — or at least some nonlinear mechanism — for purely linear processes will never reveal them. The multiplicative process in surface



**Figure S40.** Here the three blacks of eq. (S12) and their negated versions are used to prepare extreme sources and extreme reflectances. At left all sources are combined with all reflectants. Notice that most of the action is on the diagonal. At right we show the matrix of correlation coefficients of the metameric blacks and their negations (fig. S37). Apparently, in order to have an effect, source spectra and reflectance spectra need to correlate significantly.

scattering, followed by an averaging by retinal absorption, is just a kind of correlation mechanism. Figure S40 has a demo.

When mixing stuffs characterized by canonical RGB spectra one obtains unique results. One has a well defined map  $\mathbb{T}^2 \mapsto \mathbb{S}^1$ . Metamerism changes this essentially (fig. S41).



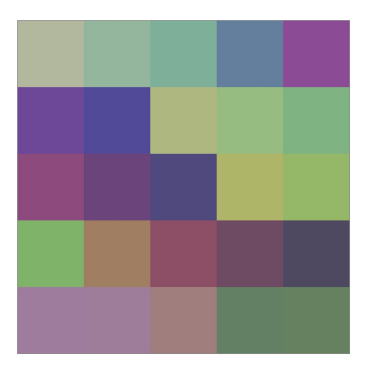


Figure S41. Mixtures of  $\sharp$ gray (RGB[50|50|50]) with  $\sharp$ gray (RGB[50|50|50]). Of course, the expectation is  $\sharp$ gray (RGB[50|50|50]). That is because mixing some stuff with itself is hardly going to change it! But, due to metamerism, not all  $\sharp$ grays have the canonical spectral reflectance factor of RGB[50|50|50], a fact that remains hidden to the senses. So multiplicative mixture may serve to distinguish identical  $\sharp$ grays as different stuffs. In this example the source spectrum was  $\mathcal{E}(\lambda)$  throughout. (At left the extreme colors obtained by "mixing gray with gray.") There are numerous grays that look the same, but are different. This is an extreme example. Ecological factors greatly reduce surprises.

The figure shows the worst case expectation for mixtures of gray with gray, observed under the standard source  $\mathcal{E}(\lambda)$ . This is evidently an intuitively magical result: one starts with two cans of paint that appear identically gray. When mixing them one obtains a chromatic color! Any hue may be obtained in such a way.

## 15 THE GRAININESS OF HUMAN PERCEPTION

Human perception is great, but — of course — the eye is far from being a spectrophotometer. The literature cites discrimation data, apparently humans may discriminate at least forty million colors!

Such numbers are useless for most application in image science. The more practical value is roughly 200–2000, depending on the operationalization.

The confusion ellipsoids shown in fig. S42 are for color reproduction with a color picker in s short-time memory condition.<sup>36</sup> The fuzziness translates to roughly a 10% fuzziness in the RGB coordinates, corresponding to about a thousand distinct colors.

<sup>&</sup>lt;sup>36</sup> J.J.Koenderink, A.J vanDoorn and K.Gegenfurtner (2018). *Graininess of RGB–Display Space. i–*Perception, 9(5), 1–46.

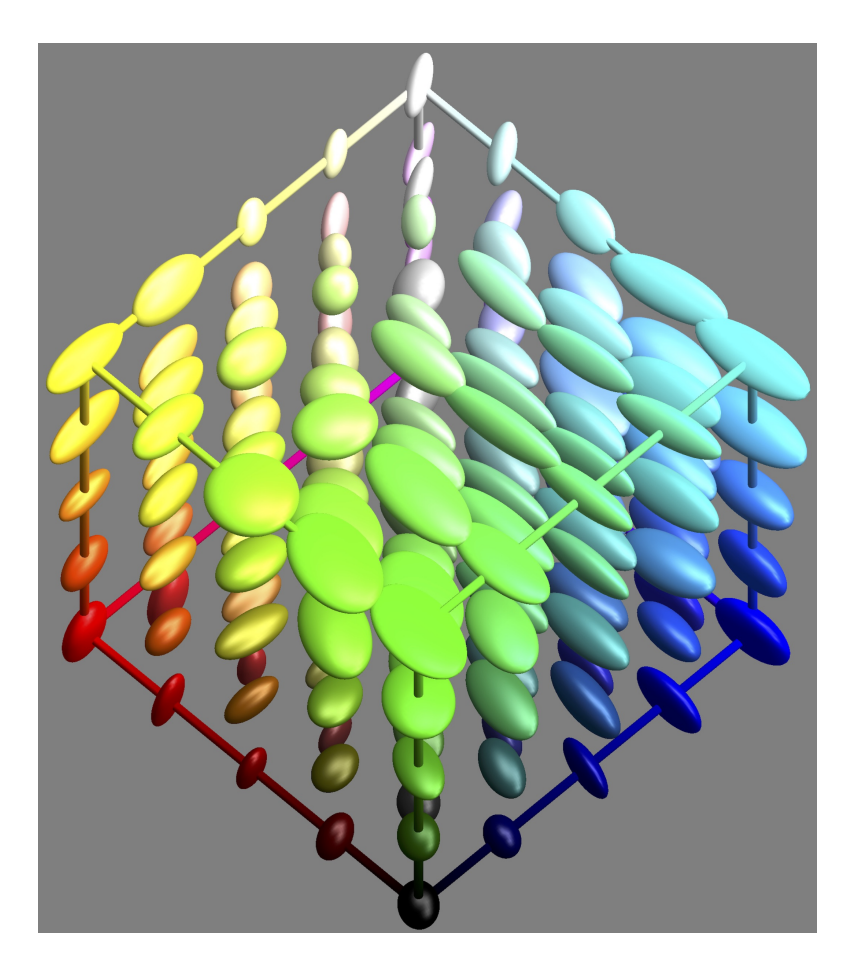


Figure S42. Empirical fuzziness of human perception.

# 16 PROBABILITY DISTRIBUTIONS OF COLORIMETRIC COORDINATES

The colorimetric coordinates are linearly related to the *product* of a spectral irradiance and a spectral reflectance factor. Thus we need to be able to deal with the statistics of products of variables. These variables may be variously distributed, here we consider uniform and normal distributions.

Spectral irradiances are non-negative quantities. In practice, they tend to be normalized by letting the unit albedo surface yield a reference.

Spectral reflectance factors are constrained to the unit interval.

For minor variations one may model distributions as normal variates, for major variations the physical constraints come into play. Thus the distributions one needs to deal with range from uniform distributions on finite intervals to normal distributions on — for all practical purposes — infinite intervals.

We cover the important cases here by regarding products of samples from uniform distributions on finite intervals and products of samples from normal distributions on the real line.

#### 16.1 Uniform distributions on the unit interval

The probability distribution function of the product of two uniform variates on the unit interval is (fig. S43 left)

$$P(x) = -\frac{\log|x|}{2},\tag{S13}$$

where one has  $P(0) = \infty$  and  $\int_{-1}^{+1} P(x) dx = 1$ . The moments are

$$m_k = \frac{1 + (-1)^k}{2(1+k)^2},\tag{S14}$$

thus the variance is 1/9, the standard deviation 1/3. The excess kurtosis is

$$\frac{m_4}{m_2^2} - 3 = 0.24, (S15)$$

thus the distribution is somewhat heavy-tailed.

The cumulative distribution function is (fig. S43 right)

$$C(x) = \frac{1}{2} (1 + x - x \log(|x|)), \qquad (S16)$$

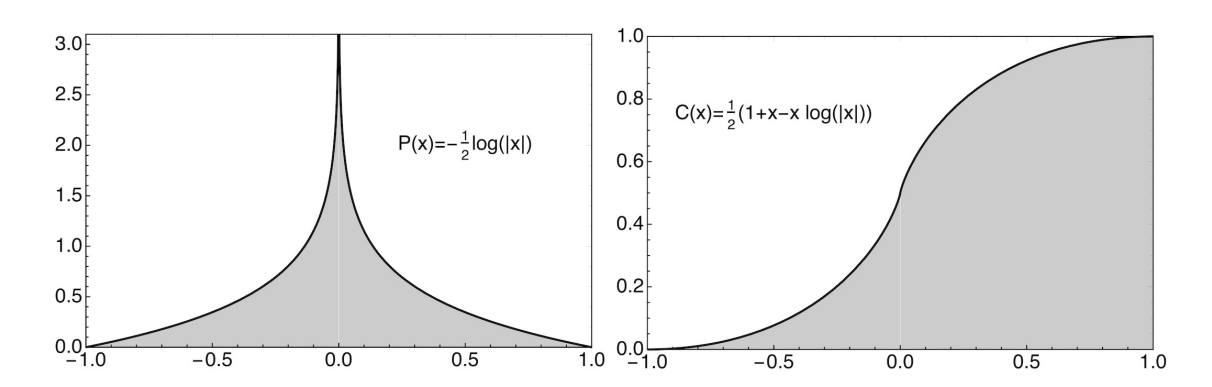


**Figure S43.** At left the probability density function for the product of two variates from the uniform distribution on the unit interval. At right the cumulative distribution. It has an infinite derivative at the origin, as the PDF has an infinite peak.

which can be inverted to find the quantile function

$$Q(x) = \frac{1 - 2x}{W_{-1}(-\frac{|2x-1|}{e})}$$
 (S17)

 $(W_{-1}$  the product-log function).

Thus the interquartile range is  $-2(W_{-1}(-1/(2e)))^{-1} \approx 0.7467...$ , only somewhat larger than twice the standard variation  $(2/3 \approx 0.6667...)$ .

### 16.2 Normal distributions of unit variance and zero mean

The probability distribution function of the product of two uniform variates of unit variance is (fig. S44 left)

$$P(x) = \frac{K_0(|x|)}{\pi},$$
 (S18)

 $(K_n \text{ a modified Bessel function of the second kind) where one has } P(0) = \infty \text{ and } \int_{-1}^{+1} P(x) \, \mathrm{d}x = 1.$  The moments are

$$m_k = \frac{2^{-1+k}(1+(-1)^k)\Gamma(\frac{1+k}{2})^2}{\pi},$$
 (S19)

thus the variance is 1 and so is the standard deviation. The excess kurtosis (as in eq. (S15)) is 6 thus the distribution is rather heavy-tailed.

The cumulative distribution function is ( $L_n$  the modified Struve function, fig. S44 right):

$$C(x) = \frac{1}{2} \left( 1 + x \left( L_{-1}(x) K_0(|x|) + L_0(|x|) K_1(|x|) \right) \right).$$
 (S20)

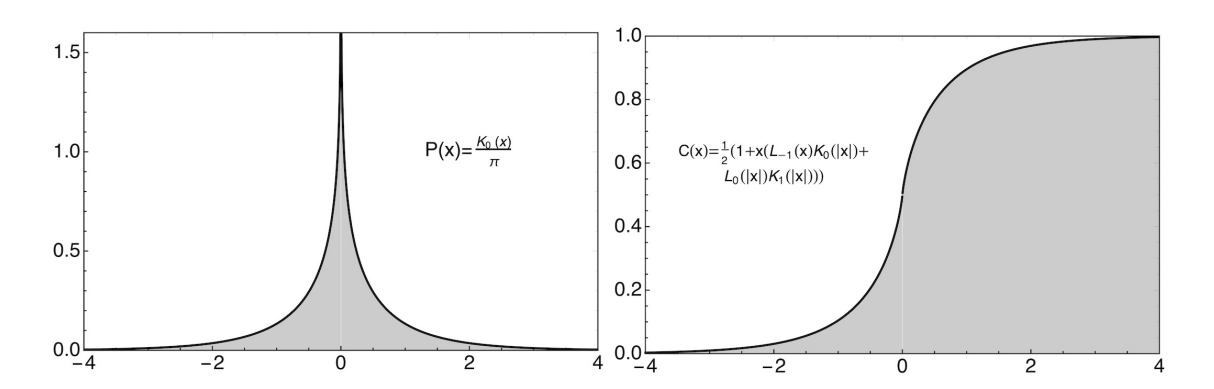


**Figure S44.** At left the probability density function for the product of two variates from the central, normal distribution of unit variance. At right the cumulative distribution. It has an infinite derivative at the origin, as the PDF has an infinite peak.

We have not been able to invert the cumulative distribution function, so we only have the quantile function in numerical approximation. The interquartile range turns out to be 0.7303..., quite a bit smaller than twice standard deviation (2). The quantile-quantile plot ("QQ-plot") illustrates the kurtotic nature of the distribution (fig. S45).

Adding multiple samplings again moves the distribution closer to normality. For instance the sum of two samples follows a Laplace distribution, thus halving the excess kurtosis. The distribution of the sum of n samples is

$$P_n(x) = \frac{2^{\frac{1-n}{2}} |x|^{\frac{1-n}{2}} K_{\frac{1-n}{2}}(|x|)}{\sqrt{\pi} \Gamma(\frac{n}{2})}.$$
 (S21)

The moments of order m are

$$m(n,m) = \frac{2^{m-1} \left(1 + (-1)^m\right) \Gamma(\frac{1+m}{2}) \Gamma(\frac{n+m}{2})}{\sqrt{\pi} \Gamma(\frac{n}{2})},$$
 (S22)

from which one sees that  $m(\infty,4)/m(\infty,2)^2-3=0$ , thus the kurtosis approaches that for a normal distribution. Indeed, for the sum of two samples the excess kurtosis is already cut by half (the Laplace distribution) and for the sum of six samples the excess kurtosis is down to 1. (Figure S46.)

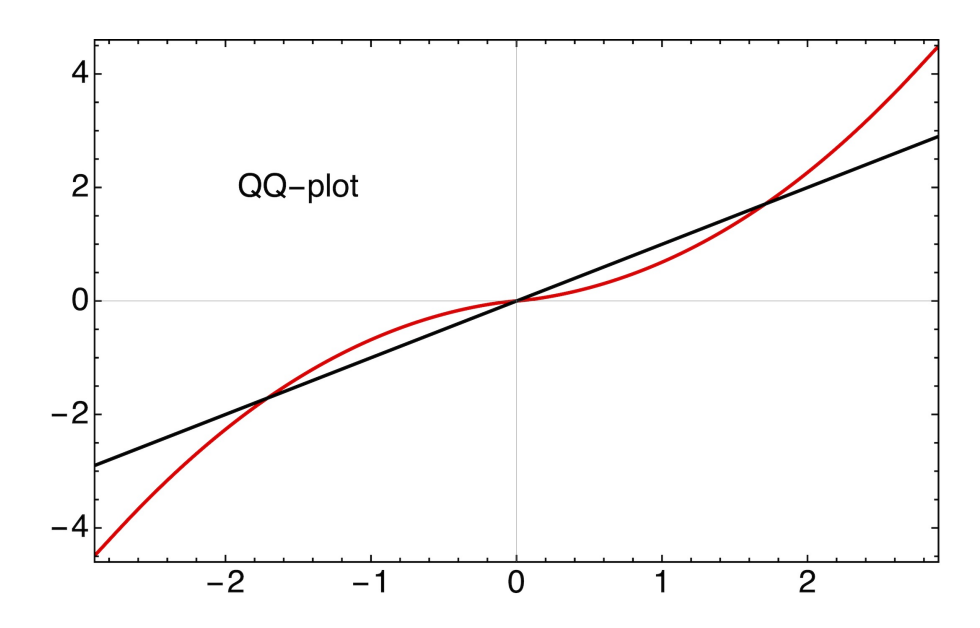


**Figure S45.** This is a QQ-Plot of the distribution shown in the previous figure. It is apparently quite kurtotic. Indeed, the kurtotic excess equals six.

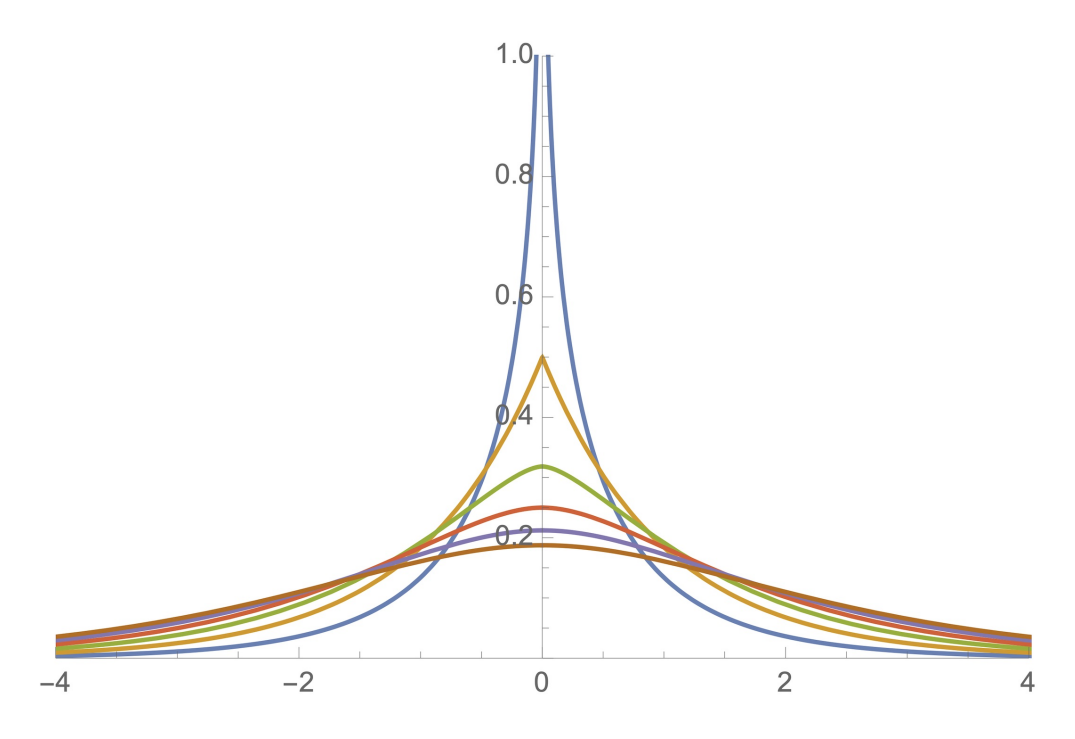


**Figure S46.** Distributions of various sums of products of normal variates. As the number of summands grows, the distribution tends to normality. For a number of three one obtains the Laplace distribution.

### 17 PREPONDERANCE OF TEAL-ORANGE OVER PURPLE-GREEN

A frequently encountered covariance structure for the RGB–coordinates in photographs of natural scenes is  $C = \begin{pmatrix} 1 & 1-\xi & 1-2\xi \\ 1-\xi & 1 & 1-\xi \\ 1-2\xi & 1-\xi & 1 \end{pmatrix}$  with  $\xi \approx 0.1$  (see also section 12). This has the effect that one is more likely to encounter a color in the teal-orange family than one in the purple-green family. The ratio of teal-orange to purple-green colors tends to 3 when color coordinates are drawn from such a multivariate normal distribution.

Another way to approach the issue is through the analysis of databases of spectral reflectances. This often yields even larger ratios.

We present an example in fig. S47. This database contains over seven-hundred items. The database contains a large variety of pigments both organic and anorganic, primarily intended as artist's colors. It is representative of many of a large variety of spectral databases we have investigated.

After deleting essentially achromatic items (color content less than 10%) we are left with 455 items. For this database the teal-orange family is 7.8 times more abundant than

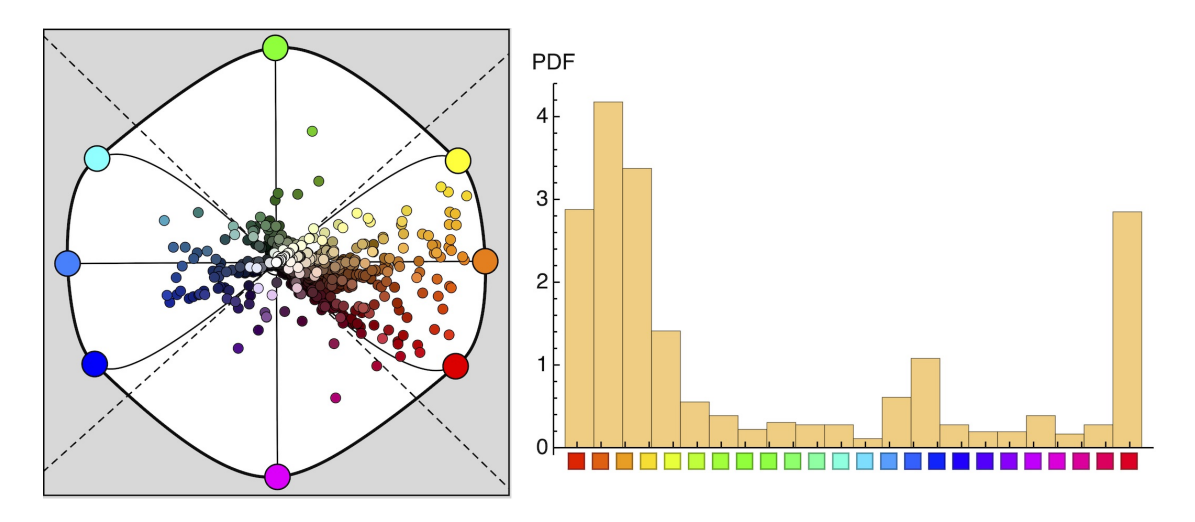


**Figure S47.** At left the chromaticities of samples of the "Kremer data base," a large data base of pigments, mainly aimed at the visual arts (data from the laboratory of the third author). The samples were sorted with respect to achromatic content, so occlusions yield something of a third dimension. Note that most chromatic contents are not very large. Note also that the distribution is far from isotropic (histogram at right). The teal-and-orange family hugely dominates the purple-green family, with orange far in the lead. This general pattern is evident in all date bases we analyzed. The causes are partly generic physics, partly ecological.

the purple-green family. Oranges are 6.3 times more abundant than teals, greens 1.3 times more abundant than purples. This appears to be fairly generic. <sup>37</sup>

That the oranges are far more abundant than the teals is due to the fact that the average spectral slope is not zero. This is the case for all data bases of "natural" reflectance factors that we have been able to study. This effect is also very marked in the statistics of pixel values in images of natural scenes. Thus far, we have not found a fitting argument from fundamental physics, it may be due to the chemical constitution of ecologically abundant biological materials and minerals.<sup>38</sup>

The same analysis can be performed on a database that only contains *colors*, not spectral reflectance factors. And example is the Resene database of paint colors. Resene Paints Limited, New Zealand's largest privately-owned and operated paint manufacturing company, has generously made their "Resene RGB Values List" available to the public. The database contains 1383 colors. Again, we see (fig. S48) the strong preference for teal—orange as compared to purple-green (factor 3.2), with orange in the lead over teal (factor 2.5).

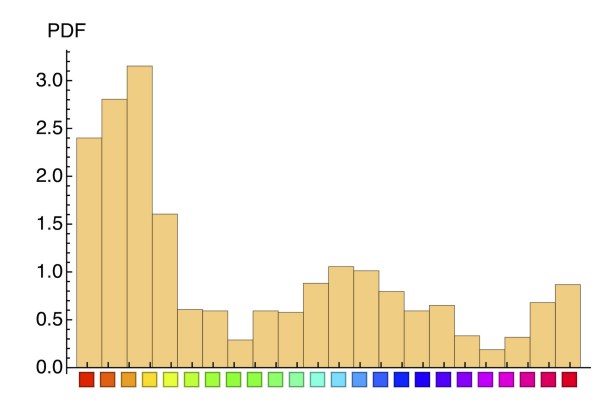


**Figure S48.** The same statistics as in figure S47 for the Resene database of paint colors.

This suggests that one might just as well use RGB images as databases. We show an example for a photograph of a tundra landscape (fig. S49). It has the right ecology for early man living in current Europe. This image contains 13 996 800 pixels, so it is a huge database.

<sup>&</sup>lt;sup>37</sup> See: J.J.Koenderink and A.J.van Doorn (2020). *Orange & Teal*. Art & Perception, in press.

<sup>&</sup>lt;sup>38</sup> See: J.J.Koenderink and A.J.van Doorn (2017). *Colors of the sublunar. i-*Perception, 8(5).

J.J.Koenderink, A.J. van Doorn and K.Gegenfurtner (2020). Colors and things. i-Perception 11(5), 1-43.

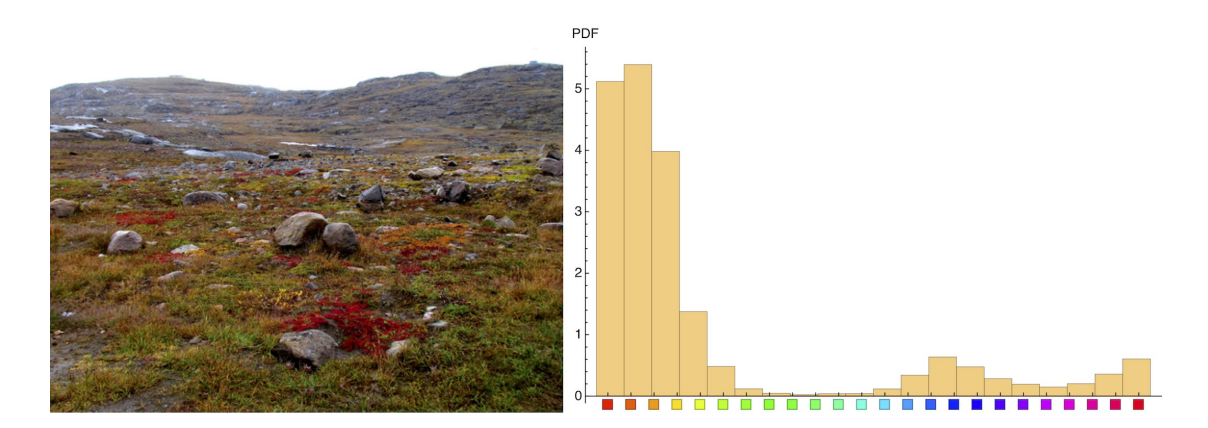


**Figure S49.** The same statistics as in figure S47 for the pixels of the Tundra image (Nunavut tundra, 7 September 2011, 15:56:18, author A.Dalia, https://en.wikipedia.org/wiki/Canadian\_Arctic\_tundra).

The correlation matrix is

$$\begin{pmatrix} 1 & 0.93 & 0.86 \\ 0.93 & 1 & 0.93 \\ 0.86 & 0.93 & 1 \end{pmatrix}, \tag{S23}$$

which is just the pattern mentioned earlier. Apparently  $\xi \approx 0.07$ . One finds this structure again and again. It is apparently not due to the particular instance, but it must be an ecological invariant.

For the distribution of hues we find a similar pattern. Teal-orange wins from purple—green by a factor of 10.4. Orange beats teal by a factor of 9.9. That these factors are extreme as compared to the previous cases may be due the preponderance of organic materials, whereas the two previous databases were due to mineral pigments and some artificial chemical compounds.

From these observations we draw an important conclusion:

- 1. The abundancies of the families of reflectance spectra teal (short pass), orange (long pass), green (band pass) and purple (band stop) can be estimated from RGB images. It is not necessary to use hyperspectral images;
- 2. These abundancies hardly depend upon the particular instance. They conform to a fundamental ecological invariant that applies to daytime scenes of the natural environment. It is found both for mineral and for organic materials;
- 3. The fact that the invariance pertains to a very diverse set of materials implies that it has to be due to a general constraint on the ecological optics;
- 4. The overwhelming abundancy oft teal—oranges means that most spectral relectances are shortpass or long pass, whereas bandpass or bandstop spectra are rare;

5. The fact that spectral slope is far more important than spectral curvature implies that the correlation length of the spectral envelope of spectral reflectance factors is at least two times (probably more) longer than the width of the visual range (about 200nm). It is in the range 400–1000nm.

These are strong conclusions from an essentially simple observation.

We can draw such conclusions due to an understanding of the relation between object colors and spectral reflectance functions (material properties). It reveals some of the power of our account of colorimetry presented in the article.

An alternative — perhaps more intuitive – way to put it is to say that RGB colors are nothing but coarse-grained spectral reflectance factors. Naturally, such a statement needs considerable unpacking — as provided in the article.